

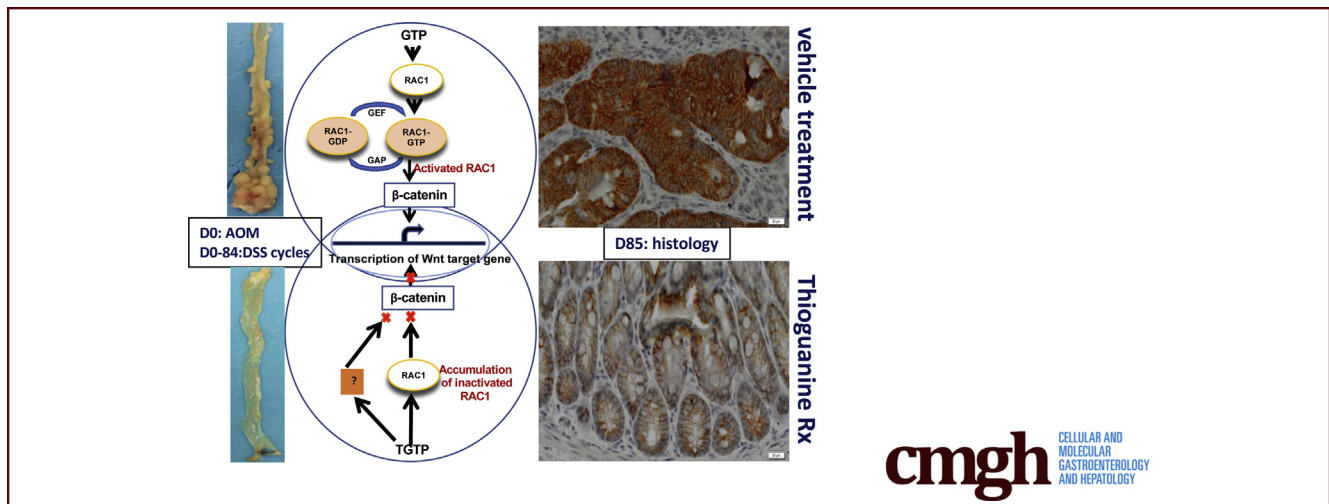
ORIGINAL RESEARCH

A Nucleotide Analog Prevents Colitis-Associated Cancer via Beta-Catenin Independently of Inflammation and Autophagy



Yong Hua Sheng,^{1,2} Rabina Giri,¹ Julie Davies,¹ Veronika Schreiber,¹ Saleh Alabbas,¹ Ramya Movva,¹ Yaowu He,³ Andy Wu,⁴ John Hooper,³ Brett McWhinney,⁵ Iulia Oancea,⁶ Gregor Kijanka,⁷ Sumaira Hasnain,² Andrew J. Lucke,⁹ David P. Fairlie,⁹ Michael A. McGuckin,⁸ Timothy H. Florin,¹ and Jakob Begun^{1,2,6}

¹Inflammatory Bowel Diseases Group, Mater Research Institute – University of Queensland, Translational Research Institute, Woolloongabba, Queensland; ²Inflammatory Disease Biology and Therapeutics Group, Mater Research Institute – University of Queensland, Translational Research Institute, Woolloongabba, Queensland; ³Cancer Biology Group, Mater Research Institute-University of Queensland, Woolloongabba, Queensland; ⁴Bones and Immunology Group, Mater Research Institute – University of Queensland, Translational Research Institute, Woolloongabba, Queensland; ⁵Queensland Pathology Services, Herston; ⁶School of Clinical Medicine, Faculty of Medicine, University of Queensland; ⁷Immune Profiling & Cancer Group, Mater Research Institute – University of Queensland, Translational Research Institute, Woolloongabba, Queensland; ⁸Faculty of Medicine Dentistry and Health Sciences, University of Melbourne, Parkville, Victoria; and ⁹ARC Centre of Excellence in Advanced Molecular Imaging, Institute for Molecular Bioscience, University of Queensland, Brisbane, Queensland, Australia



SUMMARY

Colitis increases the risk of bowel cancer. We show in mouse models that a thioguanine nucleotide can inhibit Wnt/ β -catenin signaling via Rac1 in colonic epithelial cells to prevent carcinogenesis. The novel mechanism is independent of inflammation and autophagy.

BACKGROUND & AIMS: Chronic bowel inflammation increases the risk of colon cancer; colitis-associated cancer (CAC). Thiopurine treatments are associated with a reduction in dysplasia and CAC in inflammatory bowel disease (IBD). Abnormal Wnt/ β -catenin signalling is characteristic of >90% of colorectal cancers. Immunosuppression by thiopurines is via Rac1 GTPase, which also affects Wnt/ β -catenin signalling. Autophagy is implicated in colonic tumors, and topical delivery of the thiopurine thioguanine (TG) is known to alleviate colitis and augment autophagy. This study investigated the effects of TG in a murine model of CAC and potential mechanisms.

METHODS: Colonic dysplasia was induced by exposure to azoxymethane (AOM) and dextran sodium sulfate (DSS) in

wild-type (WT) mice and mice harboring intestinal epithelial cell-specific deletion of autophagy related 7 gene (*Atg7^{ΔIEC}*). TG or vehicle was administered intrarectally, and the effect on tumor burden and β -catenin activity was assessed. The mechanisms of action of TG were investigated in vitro and in vivo.

RESULTS: TG ameliorated DSS colitis in wild-type but not *Atg7^{ΔIEC}* mice, demonstrating that anti-inflammatory effects of locally delivered TG are autophagy-dependent. However, TG inhibited CAC in both wild-type and *Atg7^{ΔIEC}* mice. This was associated with decreased β -catenin activation/nuclear translocation demonstrating that TG's inhibition of tumorigenesis occurred independently of anti-inflammatory and pro-autophagic actions. These results were confirmed in cell lines, and the dependency on Rac1 GTPase was demonstrated by siRNA knockdown and overexpression of constitutively active Rac1.

CONCLUSIONS: Our findings provide evidence for a new mechanism that could be exploited to improve CAC chemoprophylactic approaches. (*Cell Mol Gastroenterol Hepatol* 2021;11:33–53; <https://doi.org/10.1016/j.jcmgh.2020.05.012>)

Keywords: Colon Cancer; β -Catenin; Thioguanine; Autophagy.

Inflammatory bowel disease (IBD) is becoming increasingly prevalent in the developed and developing world.¹ The subgroup of IBD patients with extensive colitis has an increased risk of developing colitis-associated colorectal cancer (CAC). Although the pathogenesis of CAC in the setting of IBD is being more strongly linked to chronic inflammation and is difficult to detect endoscopically because of arising from flat dysplastic lesions,^{2,3} it has many features in common with the pathogenesis of sporadic and hereditary colon cancers, which are the second leading cause of cancer death globally.^{4,5}

Hyperactivated Wnt/ β -catenin signalling is considered a hallmark of colorectal tumorigenesis^{6–8} and has been recently implicated in immune evasion,^{9–11} invasion, and metastasis. With colorectal cancer (CRC), 90% of all tumors have a mutation(s) in the Wnt/ β -catenin pathway. However, the role of Wnt/ β -catenin signalling in CAC is less well-understood. Initial studies indicated that the Wnt/ β -catenin pathways were activated late during pathogenesis.^{12,13} However, more recent reports have suggested early Wnt/ β -catenin signalling activation^{14,15} similar to that observed in other CRCs.¹⁶ Nuclear localization of β -catenin in response to Wnt signalling, which is controlled by a large number of binding partners that include Rac1,^{17–19} is essential for its canonical signalling and similarly for the redistribution of β -catenin and T-cell factor/lymphoid enhancer factor (TCF/LEF) transcriptional activation in colon cancer cells.^{17,20}

Epidemiologic studies have shown a reduced incidence of dysplasia and CAC in those IBD patients treated with thiopurines, either azathioprine or mercaptopurine (MP).^{21–23} These are pro-drug purine base analogues, whose action is thought to relate to their conversion to active thioguanine nucleotides (TGN) in circulating activated T lymphocytes, many of which home to the gut.^{24,25} Thioguanine nucleotide triphosphate (TGTP) is the predominant intracellular species of TGN,²⁶ which binds to the small guanosine triphosphatase (GTPase) Rac1,^{24,25,27} leading to inhibition of downstream signalling (Figure 1A). The cancer chemopreventive action of thiopurines has been thought to relate nonspecifically to their overall anti-inflammatory actions.²⁸ Although MP and azathioprine (which is non-enzymatically converted to MP) are associated with reduced CAC, there are no epidemiologic data with respect to the less commonly prescribed thiopurine, thioguanine (TG).

Autophagy is an evolutionarily conserved homeostatic system that eliminates targeted cytoplasmic contents through the formation of a characteristic double-membrane autophagosome, followed by lysosomal fusion and cargo degradation. In addition to its homeostatic function, autophagy has roles in maintaining cell survival during stress and is critical in inflammation and cancer among other cellular processes. Polymorphisms in autophagy genes have been associated with IBD through genome-wide association studies.²⁹ In the context of cancer, autophagy has both antitumorigenic activity in early stages of oncogenesis where activation of autophagy can inhibit colitis and CAC initiation³⁰ and protumorigenic activity in larger tumors and metastatic disease under nutrient limiting conditions, hypoxia, and in the face of

accumulated damage to cellular organelles where autophagy is required.³⁰ ATG7 is an evolutionary conserved core autophagy protein that is essential for mammalian autophagy.³¹ Disruption of ATG7 in the intestinal epithelial cells in the murine APC^{min} model of sporadic CRC leads to decreased tumor burden in a microbiome-dependent manner due to enhanced immunosurveillance.³²

In this article, we show that TG, but not MP, acts directly on intestinal epithelial cell lines in vitro to inhibit β -catenin activity in a TGN-dependent manner. In a mouse model of CAC, daily intrarectal TG prevented colitis in wild-type (WT) mice but not in mice with deficient autophagy in intestinal epithelial cells. Administration of TG reduced CAC tumor development in both WT and autophagy-deficient mice. The largely autophagy-independent action of TG to prevent CAC involves inhibition of β -catenin signalling and its downstream nuclear translocation, which at physiological concentrations was dependent on Rac1.


Results

Thioguanine, but not Mercaptopurine, Inhibits β -Catenin Transcriptional Activity in Colonic Cell Lines

To determine whether thiopurine pro-drugs can affect β -catenin signalling, the effects of the commonly used thiopurine MP, as well as TG, were studied by using 2 cell lines, HCT116 and Caco2, harboring a β -catenin transcriptional reporter. Both cell lines, which are derived from colon cancer cells, bear an activating mutation in β -catenin. The reporter cell line cultures were exposed to TG or MP in the presence of 1 μ mol/L CHIR-99021 (CHIR) for 16 hours. CHIR stimulates the Wnt signalling pathway by inhibiting glycogen synthase kinase 3.³³ TG, but not MP, inhibited β -catenin transcriptional activity in both cell lines in a dose-dependent manner (Figure 1B). The inhibitory concentration of 50% (IC50) of TG inhibition of β -catenin transcriptional activity in these cultures was \sim 2 μ mol/L.

Immunofluorescence staining of β -catenin corroborated TG-mediated inhibition of β -catenin activity in cells with or without CHIR. The staining indicated that TG treatment markedly reduced cellular β -catenin (Figure 1C). Consistent

Abbreviations used in this paper: AOM, azoxymethane; *Atg7*^{ΔIEC}, intestinal epithelial cell-specific deletion of autophagy related 7 gene; BrdU, bromodeoxyuridine; BSA, bovine serum albumin; CAC, colitis-associated cancer; CRC, colorectal cancer; DAI, disease activity index scores; DMEM, Dulbecco modified Eagle medium; DSS, dextran sodium sulfate; GDP, guanosine diphosphate; GTP, guanosine triphosphate; GTPase, guanosine triphosphatase; HPRT, hypoxanthine phosphoribosyltransferase gene; IBD, inflammatory bowel disease; IC50, inhibitory concentration of 50%; IMPDH, inosine-5'-monophosphate dehydrogenase; MP, mercaptopurine; PBS-T, phosphate-buffered saline with 0.1% Tween-20; siRNA, small interfering RNA; TCF/LEF, T-cell factor/lymphoid enhancer factor; TG, thioguanine; TGN, thioguanine nucleotides; TGTP, thioguanine nucleotide triphosphate; WT, wild-type.

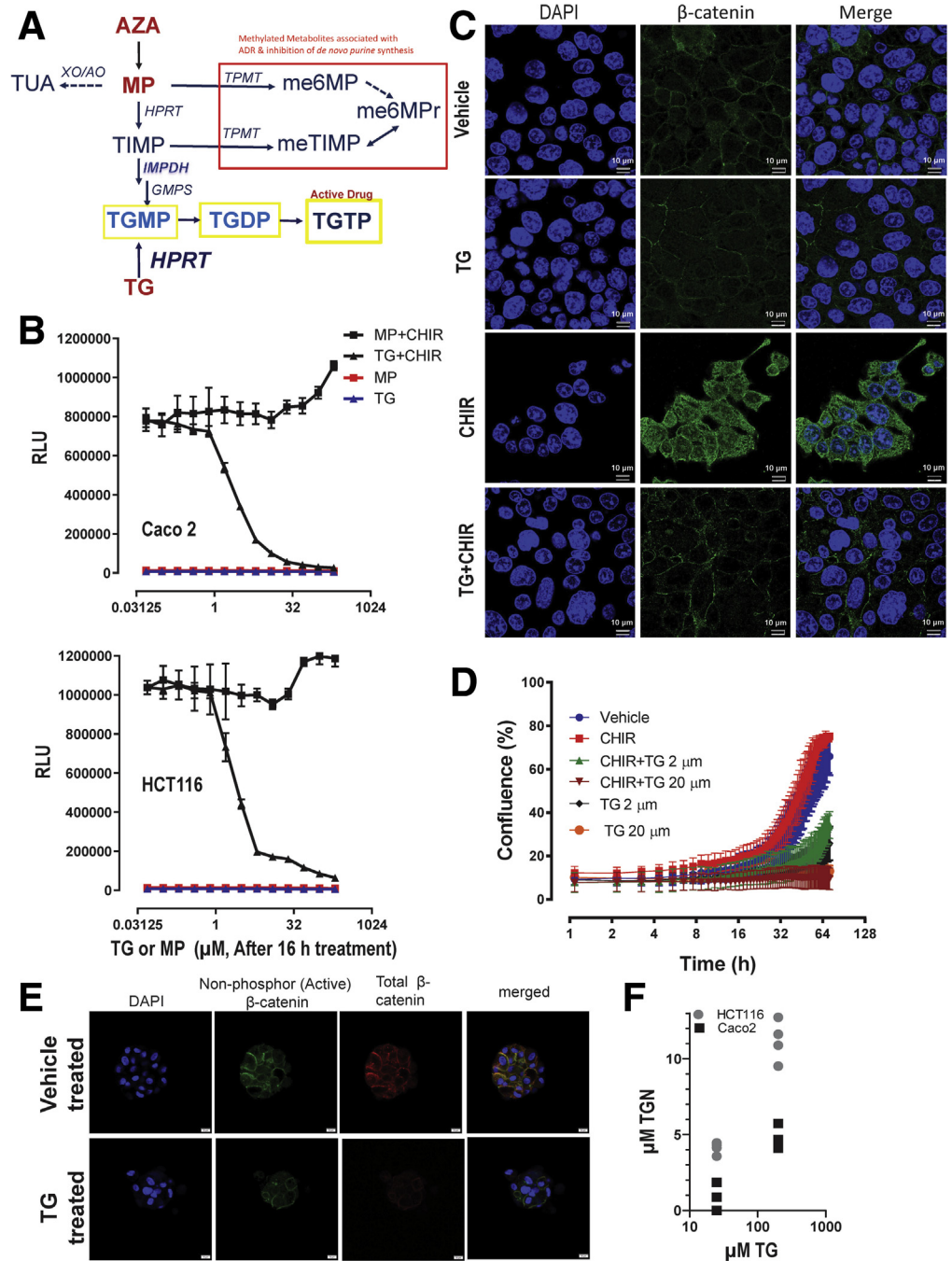
 Most current article

© 2020 The Authors. Published by Elsevier Inc. on behalf of the AGA Institute. This is an open access article under the CC BY-NC-ND license (<http://creativecommons.org/licenses/by-nc-nd/4.0/>).

2352-345X

<https://doi.org/10.1016/j.jcmgh.2020.05.012>

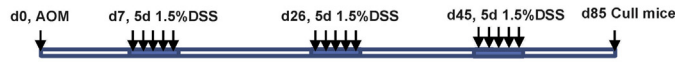
Figure 1. (A) Thiopurine pro-drug metabolism. TG and MP are purine analogue bases. Azathioprine (AZA) is non-enzymatically converted to MP. TGMP, TGDP, and TGTP are TGN. (B) TG, but not MP, inhibited β -catenin activity in vitro. β -catenin-driven transcriptional activity in HCT116 or Caco2 cells treated for 16 hours with either TG or MP in presence or absence of 1 μ mol/L CHIR-99021 (highly selective inhibitor of glycogen synthase kinase 3, which activates β -catenin by promotion of Wnt signalling), IC₅₀ TG \sim 2 μ mol/L. N = 4. (C) Immunofluorescence staining of HCT116 cells for β -catenin (green) and nuclei (DAPI, blue) \pm 5 μ mol/L TG treatment \pm 1 μ mol/L CHIR for 16 hours. Data are representative of N = 4 independent experiments. (D) Real-time imaging to 60 hours of HCT116 cells seeded into 96-well plates (7500 cells/well) by using a phase Cyte FLR live cell imager. (E) TG inhibited β -catenin in spheroid cells derived from an ulcerative colitis cancer, treated with vehicle control or TG (10 μ mol/L) for 4 days. (F) TG conversion to TGN in Caco 2 and HCT116 cell lysates. MP was not converted to TGN in the acute in vitro experiments (N = 4 at each concentration).



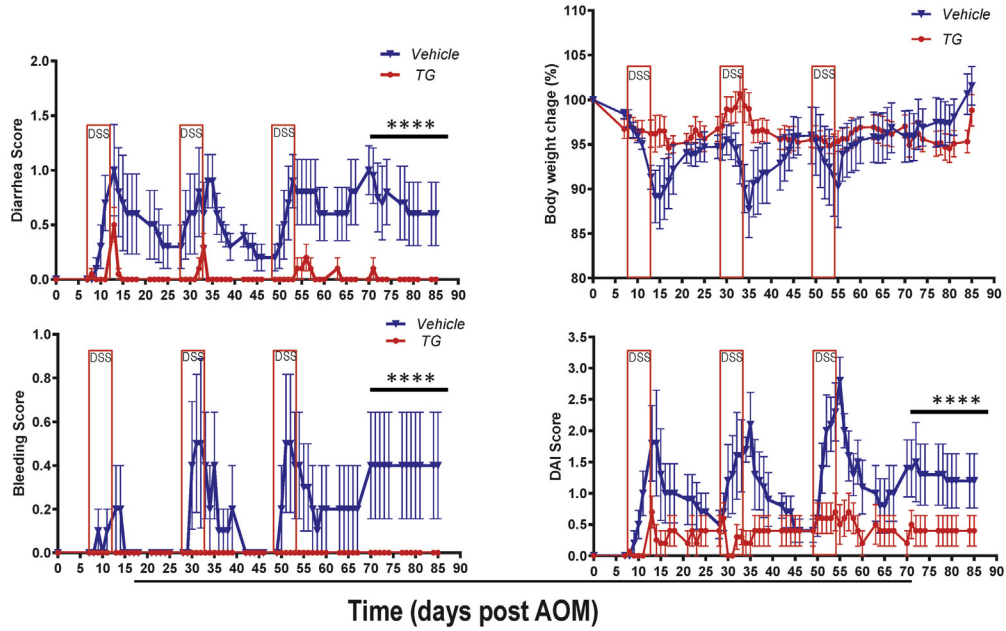
with the observation that TG inhibited Wnt signalling, TG treatment also inhibited cell proliferation in the presence and absence of CHIR stimulation in these cultures (Figure 1D). Neither MP nor TG treatment for \leq 24 hours in cultures of HCT116 or Caco2 was associated with cytotoxicity (data not shown). We subsequently had the opportunity to examine the effect of TG on epithelial spheroids grown from a colon cancer resected from a patient with pancolitis. TG inhibited both total β -catenin and activated β -catenin (Figure 1E).

TG was converted to intracellular TGN by the HCT116 and Caco2 colon cells cultures (Figure 1F). TGN were not detected in any MP cultures at similar concentrations (data not shown), which was expected because conversion of MP to TGN is rate-limited by inosine-5'-monophosphate dehydrogenase (IMPDH). These results are consistent with a requirement for TGN for the observed effect and may explain the lack of effect observed with MP treatment, because MP's, but not TG's, conversion to TGN is rate-limited by IMPDH³⁴ (Figure 1A).

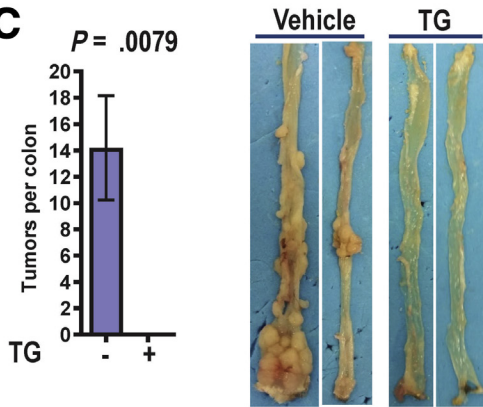
A AOM/DSS schedule for the wild type mice experiment



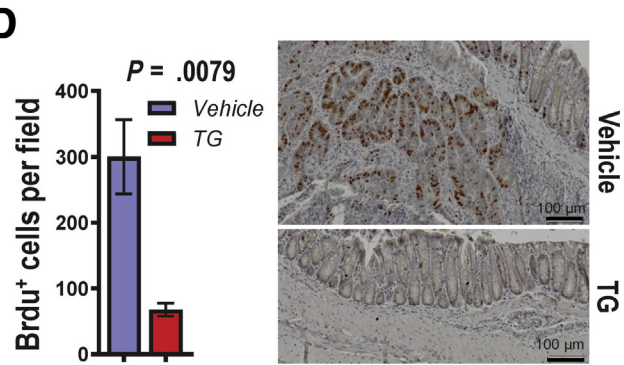
B



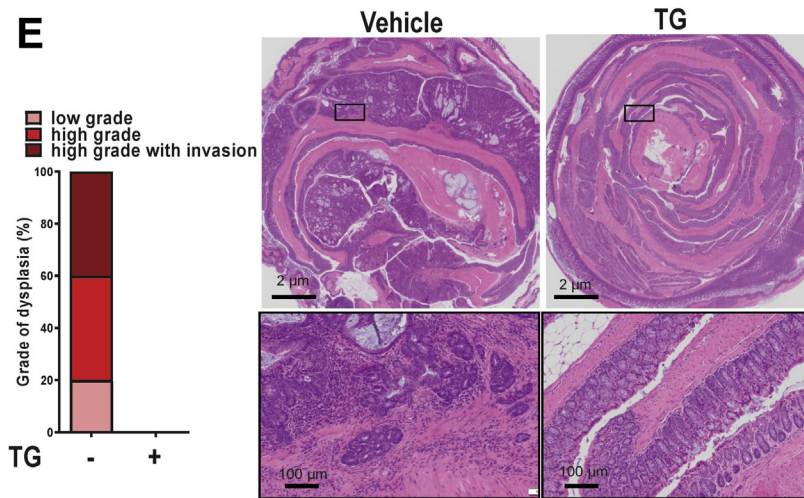
C



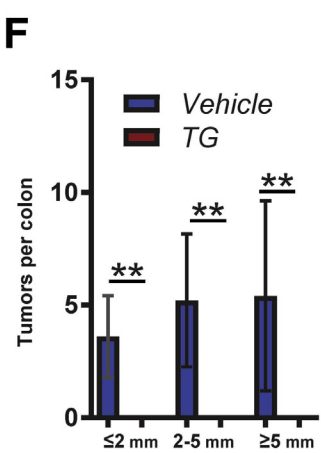
D



E



F



Intrarectal Thioguanine Inhibited the Initiation of Colitis-Associated Tumorigenesis

Having established that TG inhibits β -catenin signalling in colonic cells in vitro at an IC50 of 2 μ mol/L (0.33 mg/kg), we next ascertained the effect of TG on colon tumorigenesis in vivo by using an established mouse model of CAC induced by intraperitoneal azoxymethane (AOM) administration, followed by cycles of dextran sodium sulfate (DSS) exposure to induce colonic inflammation (Figure 2A).³⁵ To specifically examine the effect of TG on CAC oncogenesis we use localized delivery via intrarectal gavage. A large daily dose of TG 1.5 mg/kg was selected for the in vivo mouse experiments because the contact time of intrarectal drug with colonic mucosa in the mice was short because of rapid expulsion of enema fluid by the ambulant mice. Consistent with our previous findings with TG,³⁶ mice treated with intrarectal TG exhibited fewer clinical signs of colitis during and immediately after the DSS cycles than control vehicle treated mice, as evidenced by less diarrhea, absence of rectal bleeding, and lower disease activity index scores (DAI) during periods both on and off DSS treatment (Figure 2B).

Vehicle-treated mice had a mean 14 (standard error, 2.0) colonic tumors (Figure 2C). Tumors were associated with an increase in proliferating bromodeoxyuridine (BrdU) + cells (Figure 2D). Areas of high-grade dysplasia and high-grade dysplasia with tumor invasion into submucosa were twice as frequent as areas with low-grade dysplasia. Remarkably, intrarectal TG treatment completely prevented colonic tumorigenesis (Figure 2C and F). TG-treated mice had fewer proliferating (BrdU⁺) cells in comparable regions of the colon than vehicle-treated mice (Figure 2D). There were no tumors and no dysplasia in the WT mice treated with TG (Figure 2E and F).

Oncoprotection by Intrarectal Thioguanine Was Mainly Independent of Thioguanine's Effect on Autophagy

We had previously reported that TG induced a rapid augmentation of autophagy by intestinal epithelial cells in vitro,³⁶ which could contribute to how TG effects a rapid amelioration of colitis.³⁶ Under normal physiological conditions Wnt/ β -catenin signalling has been implicated in suppression of autophagy, and β -catenin is itself subject to proteasome-independent degradation by autophagy. Intestinal epithelial autophagy also impacts CRC growth once a tumor is initiated in some murine models of colon cancer.³⁰

Therefore, we investigated the role of TG in the absence of intestinal epithelial autophagy in the mouse CAC model by using conditional *Atg 7^{-/- villin:Cre}* mice with *Atg7* selectively absent in intestinal epithelial cells (*Atg7^{ΔIEC}*) (Figure 3A).

Intrarectal TG did not improve the colitis associated with exposure to each cycle of DSS in this model, as indicated by similar DAI scores in TG-treated and vehicle-treated mice (Figure 3B), which is consistent with the anti-inflammatory effect of intrarectal TG being autophagy dependent. Rectal bleeding was significantly increased in the vehicle-treated *Atg7^{ΔIEC}* mice from day 70, which was consistent with tumor formation; there was a mean of 8 tumors per colon in these vehicle-treated *Atg7^{ΔIEC}* mice. On the other hand, TG treatment was associated with a significant reduction of tumor load (<4 tumors/colon) in the *Atg7^{ΔIEC}* mice (Figure 3C; $P = .006$) despite the ongoing inflammatory burden with the TG treatment. TG-treated tumors in *Atg7^{ΔIEC}* mice had less proliferative (BrdU⁺) cells than control-treated *Atg7^{ΔIEC}* tumors (Figure 3D). Conventional H&E histopathologic assessment of intrarectal vehicle-treated *Atg7^{ΔIEC}* mice revealed less high-grade dysplasia and less high-grade dysplasia with invasion into submucosa, compared with vehicle-treated WT mice (Figures 2E and 3E). TG-treated *Atg7^{ΔIEC}* mice had low-grade dysplasia but no areas of high-grade dysplasia or invasion (Figure 3E). Whereas tumors in vehicle-treated WT mice tended to be ≥ 5 mm, those in the vehicle-treated *Atg7^{ΔIEC}* mice were mainly ≤ 5 mm. The tumors in the TG-treated *Atg7^{ΔIEC}* mice were all ≤ 2 mm (Figures 2F and 3C). Figure 3F illustrates tumor load data from the 2 experiments (Figures 2C and 3C); there was a trend for fewer tumors in vehicle-treated *Atg7^{ΔIEC}* mice compared with vehicle-treated WT mice ($P = .054$), and although TG treatment was effective in the *Atg7^{ΔIEC}* mice ($P = .003$), it was less effective in these mice compared with WT where TG treatment was associated with a complete absence of tumors.

Rectal delivery of TG was associated with scant systemic toxicity in these models; there was no evidence of hepatic sinusoidal obstructive syndrome³⁷ in any of the mice treated with daily intrarectal TG. Figure 4A shows a representative histology image from vehicle-treated and TG-treated animals. Intrarectal TG during the 85-day treatment duration in the WT mice was not associated with peripheral blood immunosuppression (Figure 4B), but mild leukopenia was demonstrated in the *Atg7^{ΔIEC}* mice at day 85 ($P < .05$). Intrarectal TG treatment did not appear to alter total mesenteric lymph node leukocyte numbers. However,

Figure 2. (See previous page). TG inhibited colitis and colitis-associated colorectal tumor development and progression in mice. (A) Scheme showing induction procedure for AOM/DSS model of CAC. C57/BL6 WT were treated with DSS 1.5% in drinking water for 5 days, 3 cycles, \pm daily intrarectal TG 1.5 mg/kg for 85 days ($N \geq 5$ each group). (B) Daily assessments in TG or vehicle-treated mice ($n \geq 5$) for diarrhea, body weight, rectal bleeding, and DAI score. (C) At death day 85: number of colon tumors (left panel); representative macroscopic images of colonic mucosa (right panel). (D) Average number of BrdU-staining cells per field of view in tumors and comparable areas of TG-treated mice, and representative immunohistochemical staining for BrdU in tumors (right panel). (E) Severity of dysplasia vs TG treatment in tumors 85 days after injection of AOM with representative H&E-stained sections of colonic tissue with tumors (scale bars are shown, right panel). (F) Tumor diameter and frequency in vehicle versus TG-treated mice. Statistics B–D and F: mean \pm standard error of the mean, Mann-Whitney *U* test. *TG vs vehicle, **** $P < .0001$ (B), ** $P < .01$ (F) are *P* values shown (C and D).

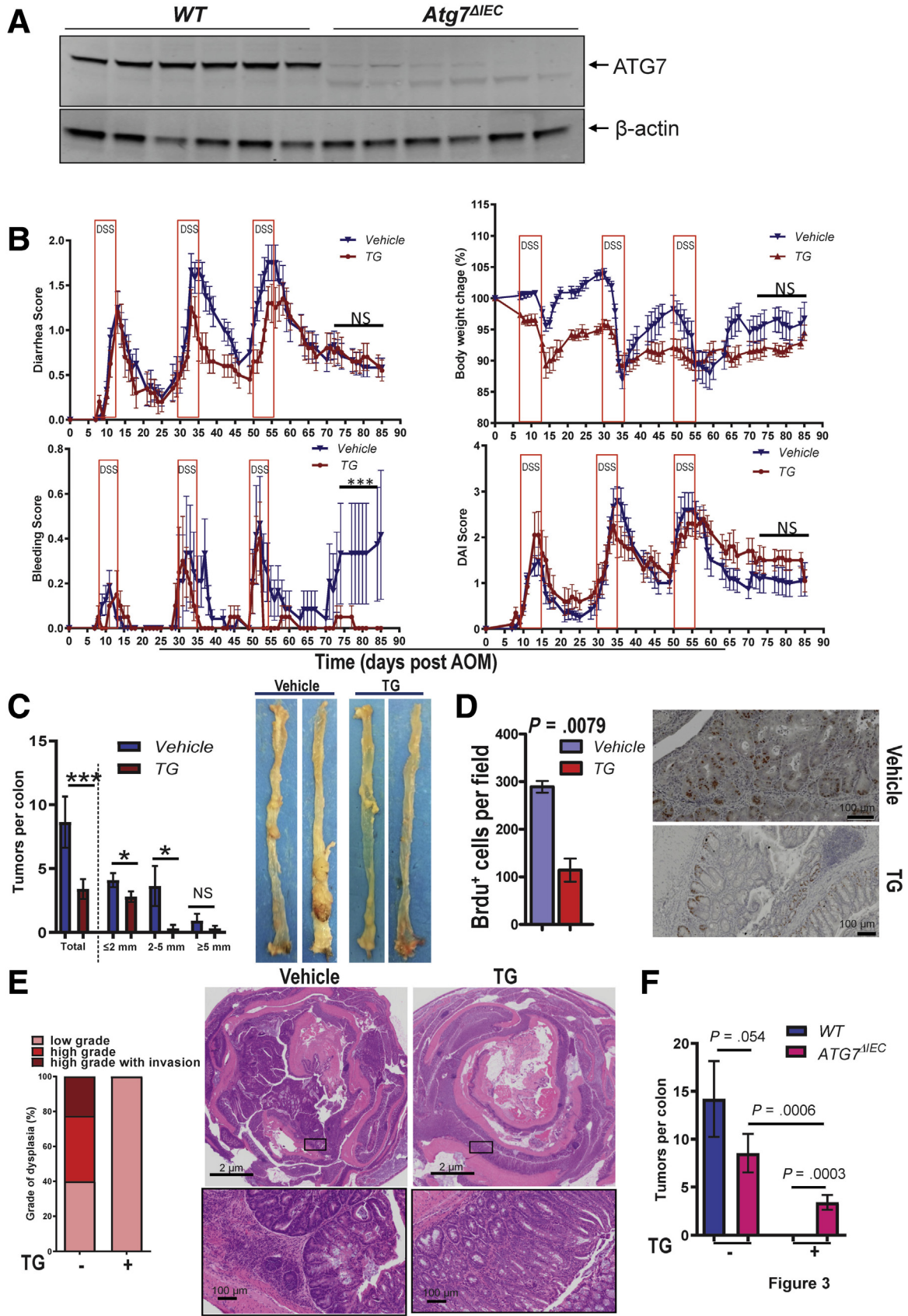


Figure 3

intrarectal TG was associated with a small but significant change in the CD4:CD8 ratio in mesenteric lymph nodes at day 85 (Figure 4C; $P < .05$).

In summary, although the size of the dose and the duration of TG administration for 85 days were significantly greater than previously reported,^{36,38} there was negligible systemic toxicity, reinforcing previous observations showing a lack of toxicity with rectally administered TG.^{36–38} The anti-inflammatory effects of rectally delivered TG in colitis is dependent on intestinal epithelial cell autophagy, a mechanism that is in addition to recognized immunomodulatory actions on adaptive T-lymphocyte-mediated immune responses and innate immunity from systemically absorbed TG.³⁶ Furthermore, inhibition of tumor formation by daily intrarectal TG is largely independent of intestinal epithelial cell autophagy, even in the absence of its anti-inflammatory effects. The lower tumor load in vehicle-treated *Atg7^{ΔIEC}* mice than in vehicle-treated WT mice is consistent with the reported role of intestinal epithelial cell autophagy in the development of CRC.³²

Thioguanine Treatment Was Associated With Decreased Beta-Catenin Nuclear Accumulation and Oncogenic Transcriptional Activity in Colitis-Associated Cancer Tumors

Because TG treatment of epithelial cells reduced β -catenin activity in vitro, we investigated the effects of TG administration on β -catenin in the CAC model. Beta-catenin in tumors was assessed by immunohistochemistry in WT mice; greater cytoplasmic staining intensity and particularly strong nuclear β -catenin localization were observed in vehicle-treated tumors compared with comparable regions in the colons of TG-treated mice in which β -catenin was typically restricted to discrete areas of the cytoplasm/cellular junctions (Figure 5A). Quantitative analysis confirmed significantly higher β -catenin staining as indicated by both staining area and intensity in vehicle-treated tumors (Figure 5A). Western blot analysis of tumor tissue from the distal colon using an antibody specific for active nonphosphorylated β -catenin confirmed higher levels in vehicle-treated tumors compared with distal colon from TG-treated mice in a similar location (Figure 5B). These data corroborate that intrarectal TG treatment inhibited activation and nuclear translocation of β -catenin in the AOM/DSS-treated mice.

To gain insight into the consequences of TG-inhibited β -catenin activity in the tumors, we assessed the relationship between β -catenin expression and expression of oncogenic target genes. Higher expression levels of cyclin D1 and C-Jun (drivers of cell cycle G1/S-phase transition and involvement in DNA damage repair), matrix metalloproteinase-7

(believed to have an oncogenic function in colonic tumorigenesis³⁹), CD44 (a marker for cancer stem cells⁴⁰), and survivin (cell survival marker^{41,42}) were generally observed within the vehicle-treated tumors (Figure 5B) in comparison with TG-treated animals. Taken together with the BrdU measurements, these results suggest that TG inhibits tumor cell proliferation and invasion by actions on β -catenin transcriptional activity and downstream target gene expression.

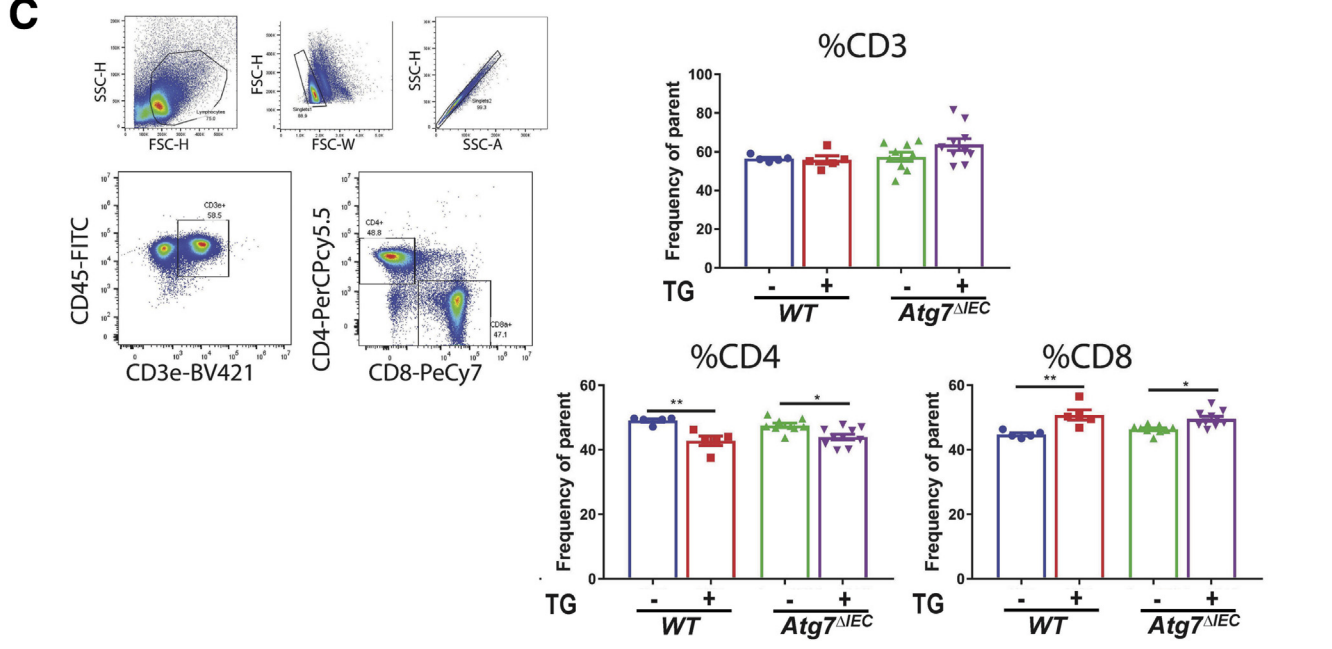
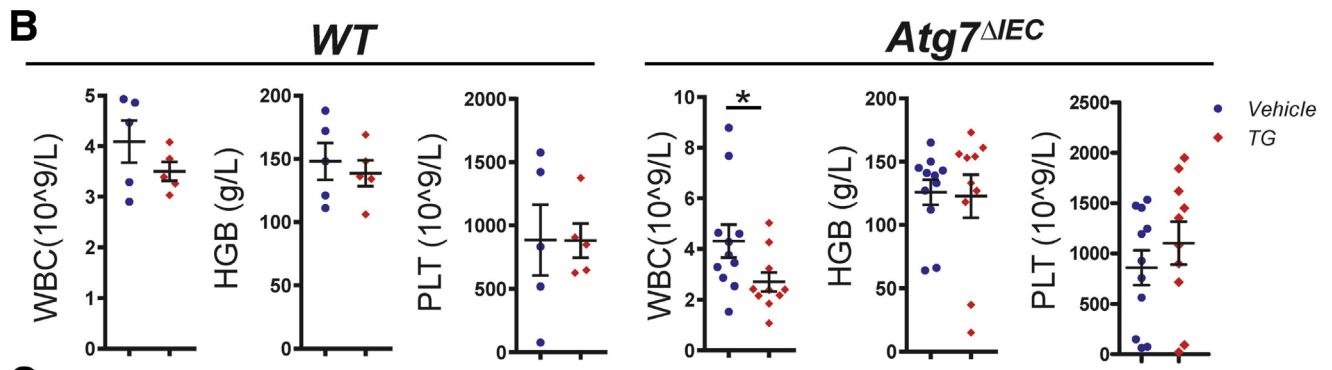
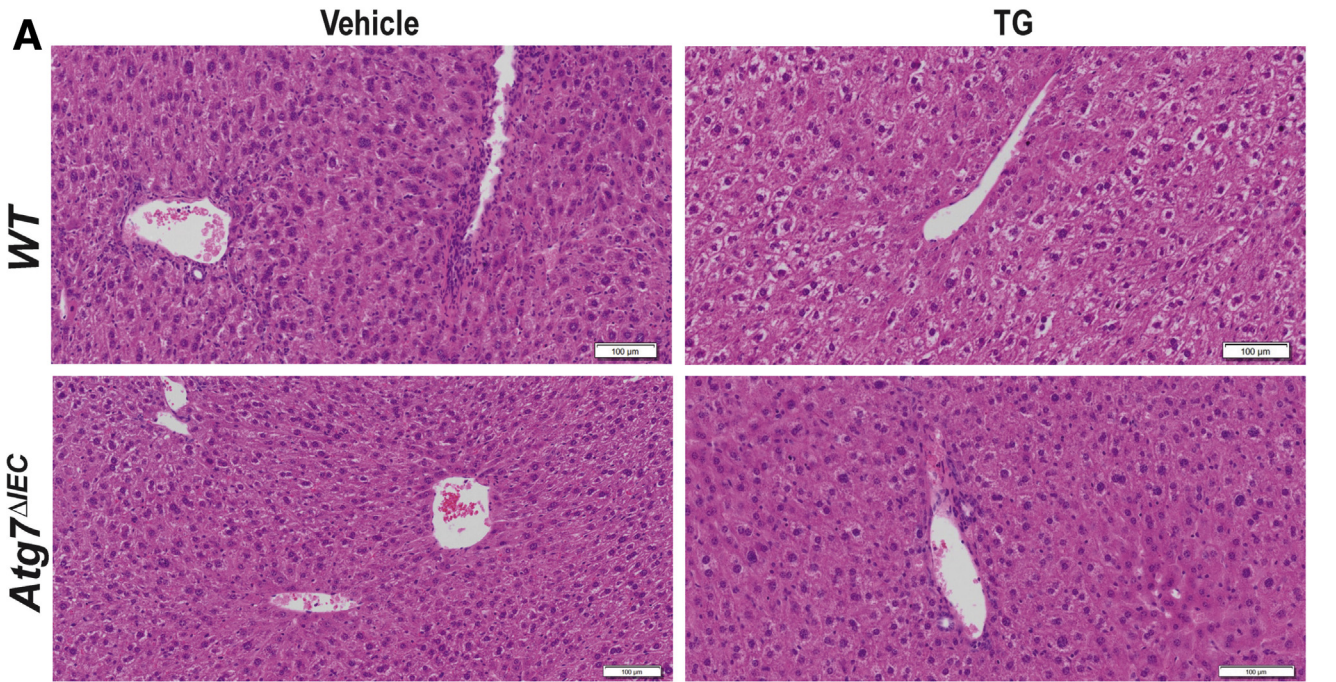
To determine whether TG also affected β -catenin activation in the setting of autophagy disruption, we further examined β -catenin levels in *Atg7^{ΔIEC}* tumors by immunohistochemistry. As with WT tumors, we found much higher cytoplasmic and particularly strong nuclear β -catenin localization in vehicle-treated tumors compared with TG-treated tumors (Figure 6A). In addition, there appeared to be more cytoplasmic β -catenin staining in TG-treated *Atg7^{ΔIEC}* tumors than in TG-treated WT tumors (Figure 6A), which is consistent with reports that intestinal epithelial cell autophagy normally downregulates cytosol β -catenin level.³⁰ Tumors in *Atg7^{ΔIEC}* mice treated with TG had markedly reduced expression of oncogenic target genes (Figure 6B). When these data are considered along with the similar measurements in WT tumors, they indicate that TG's inhibition of β -catenin oncogenic transcriptional activity is independent of autophagy.

Extending the relevance of these mechanistic findings to human cancer, we examined the effect of *ATG7* silencing on β -catenin transcriptional activity in response to TG treatment in the human colon cancer derived HCT116 and Caco2 cell lines using the luciferase reporter assay. Two independent sets of *ATG7* small interfering RNAs (siRNAs) were used to control for potential off-target effects. *ATG7* siRNA reduced *ATG7* protein expression by ~85% in Caco2 and 95% in HCT116 cell lines (Figure 7A). Similar to our in vivo finding, we noted higher β -catenin transcriptional activity in *ATG7* knockdown cells than in control cells under basal conditions (Figure 7B), which is consistent with the previously reported autophagy-mediated degradation of β -catenin⁴³; however, CHIR treatment still resulted in additional activation. Treatment with TG in conjunction with CHIR activation resulted in significantly reduced β -catenin activity in a dose-dependent manner (Figure 7C). This occurred despite knockdown of *ATG7* and was consistent with the in vivo findings of TG's oncoprotective effect being largely independent of autophagy (Figure 5).

Thioguanine Suppresses β -Catenin Activity via Conversion to Thioguanine Nucleotides

The cellular metabolism of thiopurines results in the production of many metabolites. To confirm that the action of TG in the cell lines involved TGN (Figure 1),

Figure 3. (See previous page). TG inhibited colorectal tumor development in *Atg7^{ΔIEC}* conditional knockout mice. (A) Western blotting for *ATG7* in colonic epithelial cells (IEC) to confirm deletion of *ATG7* specifically in IECs in conditional knockout mice. (B–E) ($N \geq 10$ each group) and figure legend as for Figure 2. (F) Combines data from 2E and 3C. Statistics B–D and F: mean \pm standard error of the mean, Mann-Whitney *U* test. *TG vs vehicle, *** $P < .001$, ** $P < .01$, * $P < .05$. *P* values otherwise shown.



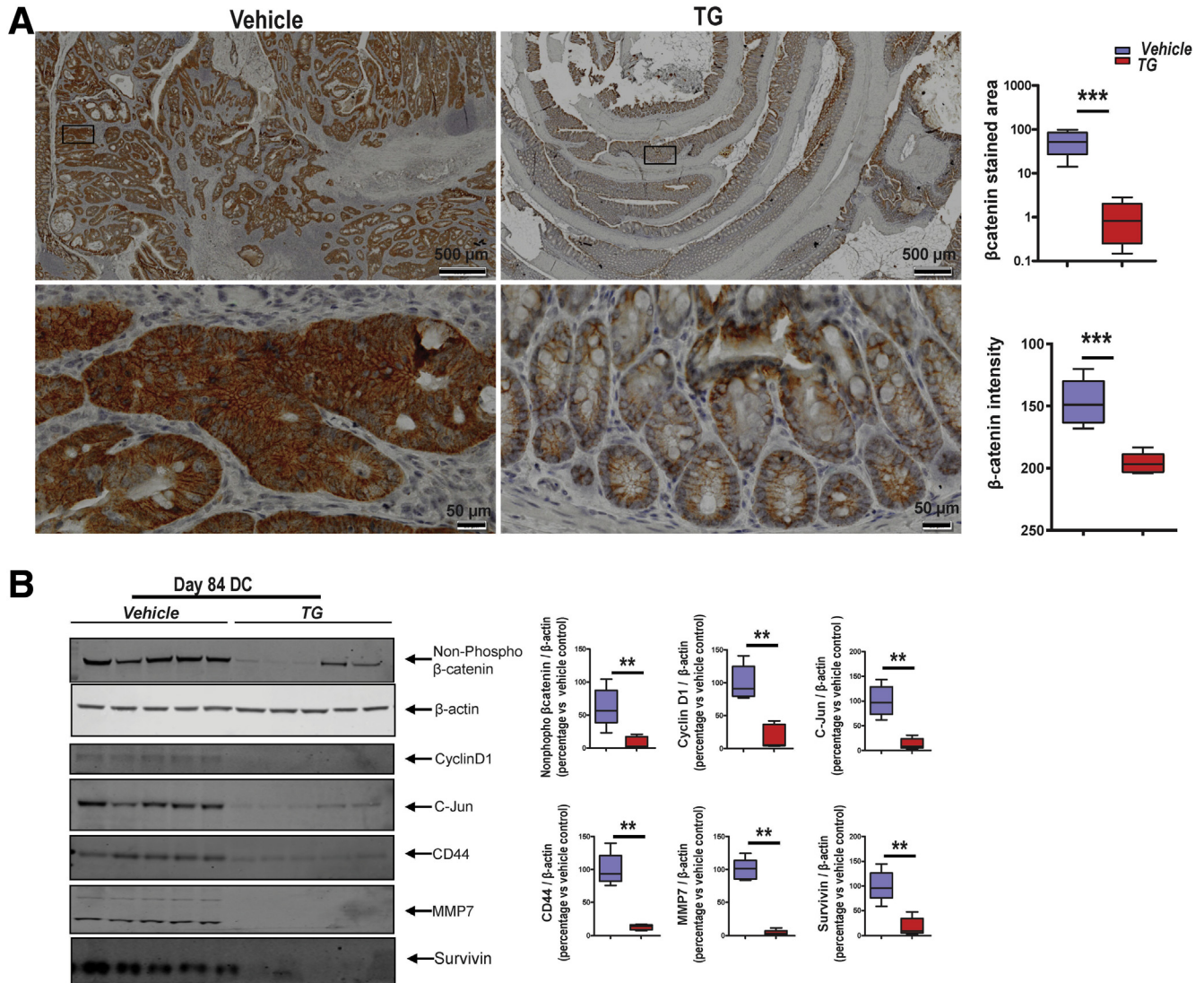


Figure 5. TG inhibited β -catenin activity in CAC tumors in vivo. Measurements in TG or vehicle-treated tumors at day 85 (N \geq 5 each group). (A) Immunohistochemical (IHC) analysis of β -catenin in WT mice and in $Atg7^{dIEC}$ conditional knockout mice. *Left panels*: representative IHC staining for β -catenin. *Right panels*: β -catenin protein levels assessed using IHC and Visiopharm software (where higher intensity has a lower value) and expressed as percentage of β -catenin positive cells within the tumors (*upper*) and tumor β -catenin intensity (*bottom*) from each mouse (5 mice per group). (B) Immunoblot analysis of non-phosphorylated β -catenin and its downstream tumor promoting gene products, cyclin D1, C-Jun, CD44, MMP7, survivin in WT mice and (C) in $Atg7^{dIEC}$ mice. *Each lane* represents distal colon or pooled tumors from distal colon in an individual mouse. Densitometry of proteins corrected for β -actin in *bottom right panel*. Statistics: *box plots* show median, quartiles, and range; Mann-Whitney *U* test. *TG vs vehicle, ***P* < .01. Data representative of 3 independent experiments.

we examined the effect of hypoxanthine phosphoribosyltransferase gene (*HPRT*) silencing on β -catenin transcriptional activity in response to TG treatment in HCT116 and Caco2 cells using the luciferase reporter assay. Disruption of *HPRT* results in an inability for

cells to metabolize TG to TGN. Two independent sets of *HPRT* siRNAs were used to control for potential off-target effects. Each set of *HPRT* siRNA reduced *HPRT* protein expression by \sim 85% in these cell lines (Figure 8A). Inhibition of β -catenin transcription activity

Figure 4. (See previous page). Long-term daily intrarectal TG treatment was not associated with clinically significant systemic toxicity. (A) Sinusoidal obstructive syndrome was not present at day 85. Representative H&E liver histology for vehicle and TG-treated animals. (B) Hematologic parameters (white blood cell counts, hemoglobin, and platelets) in peripheral blood at day 85 from WT and $Atg7^{dIEC}$ mice. (C) Fluorescence-activated cell sorter plots showing cell gating strategy and subsets of CD45+CD3e+ (T lymphocyte) and CD4+, CD8+ populations. There was a small but statistically significant increase in CD8: CD4 mesenteric node lymphocytes with TG treatment in both WT and $Atg7^{dIEC}$ mice.

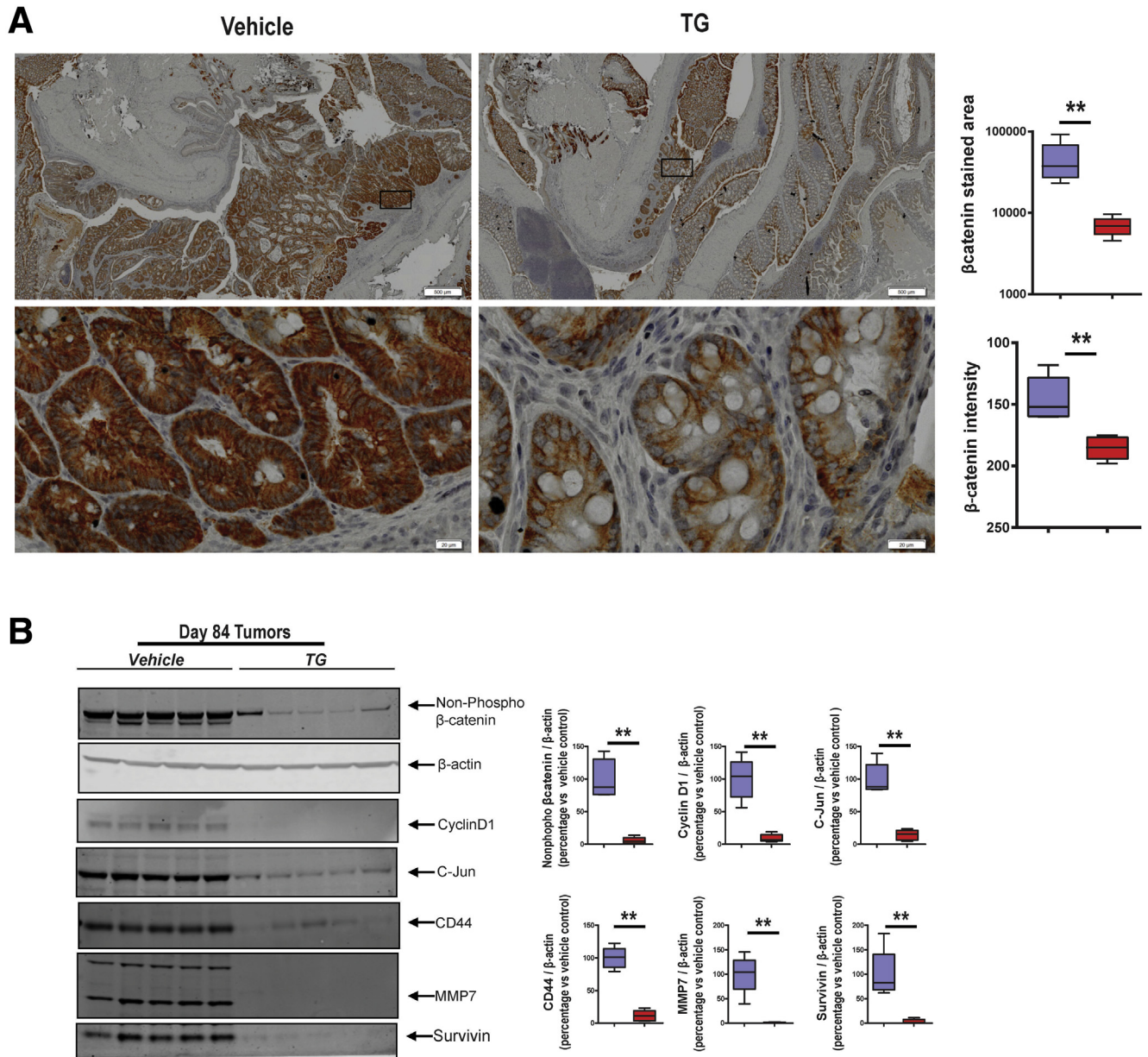


Figure 6. TG inhibited β -catenin activity in $Atg7^{AIEC}$ conditional knockout mice. Measurements in TG or vehicle-treated tumors at day 85 ($N \geq 5$ each group). (A) Immunohistochemical (IHC) analysis of β -catenin in WT mice and in $Atg7^{AIEC}$ conditional knockout mice. *Left panels*: representative IHC staining for β -catenin. *Right panels*: β -catenin protein levels assessed using IHC and Visiopharm software (where higher intensity has a lower value) and expressed as percentage of β -catenin positive cells within the tumors (*upper*) and tumor β -catenin intensity (*bottom*) from each mouse (5 mice per group). (B) Immunoblot analysis of non-phosphorylated β -catenin and its downstream tumor promoting gene products, cyclin D1, C-Jun, CD44, MMP7, survivin in WT mice and (C) in $Atg7^{AIEC}$ mice. Each lane represents distal colon or pooled tumors from distal colon in an individual mouse. Densitometry of proteins corrected for β -actin in *bottom right panel*. Statistics: *box plots* show median, quartiles, and range; Mann-Whitney U test. *TG vs vehicle, ** $P < .01$. Data representative of 3 independent experiments.

was seen in both TG-treated cells treated with control siRNA, but there was no inhibition of β -catenin with knockdown of HPRT, thus indicating that the effect was mediated by TGN (Figure 8B). To corroborate these findings we examined the effect of TG on fibroblasts harvested from $Hprt^{-/-}$ mice. Fibroblast cell cultures

derived from both WT and $Hprt^{-/-}$ mice were incubated for 16 hours with vehicle control or 10 $\mu\text{mol/L}$ TG \pm CHIR. As expected, cellular and nuclear β -catenin was significantly reduced in TG-treated WT-derived fibroblasts, but there was no effect in the absence of $Hprt$ (Figure 8C). Immunoblots confirmed decreased

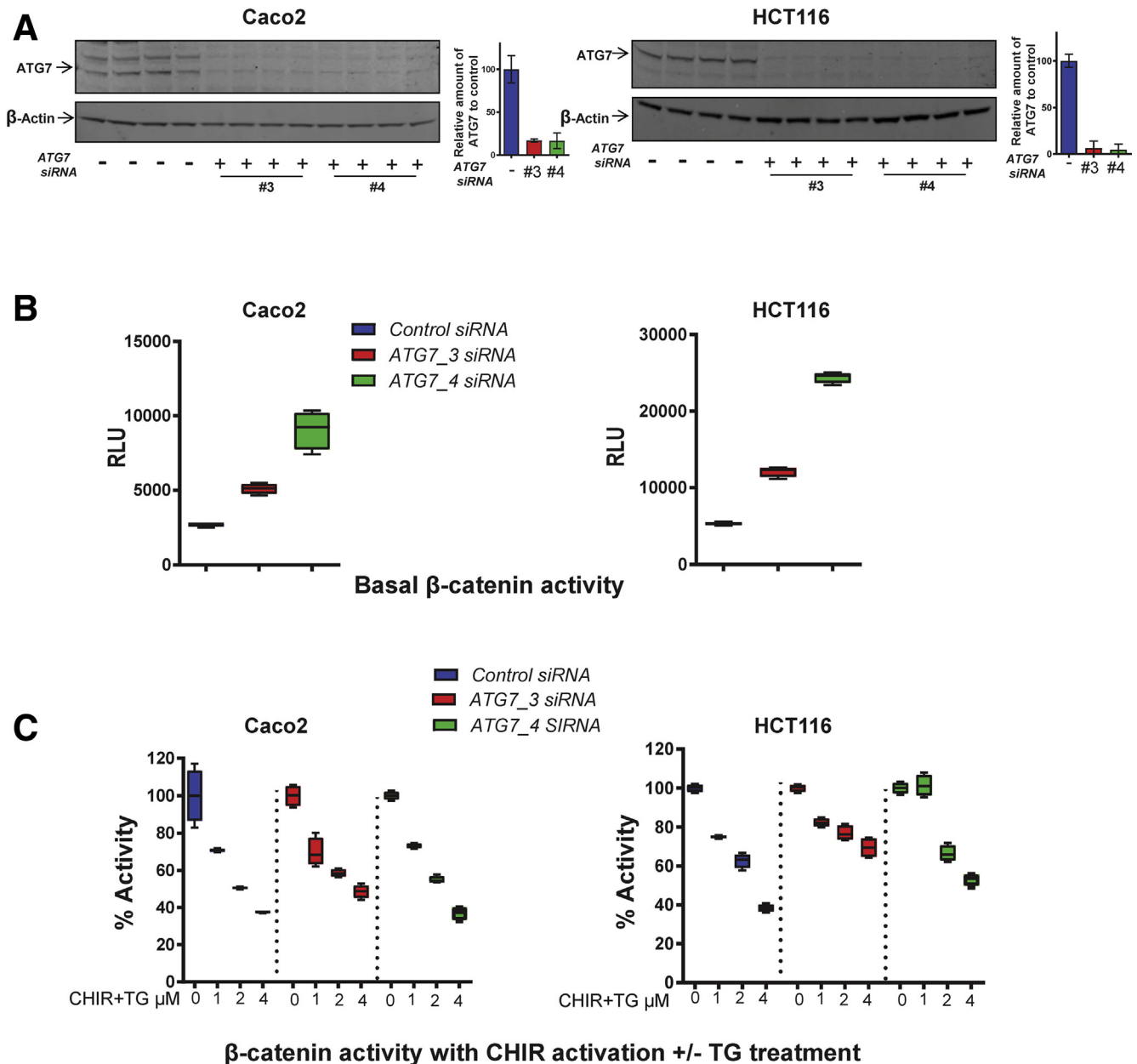
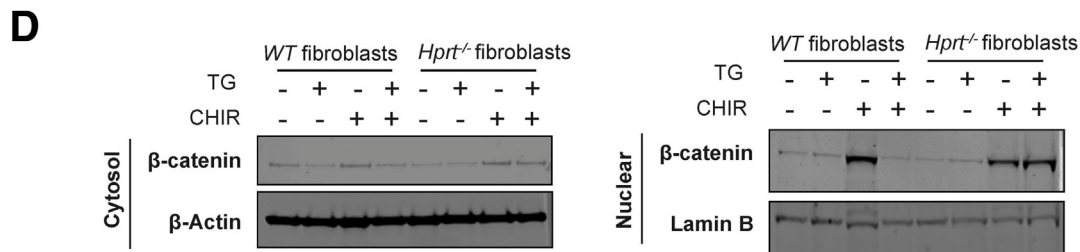
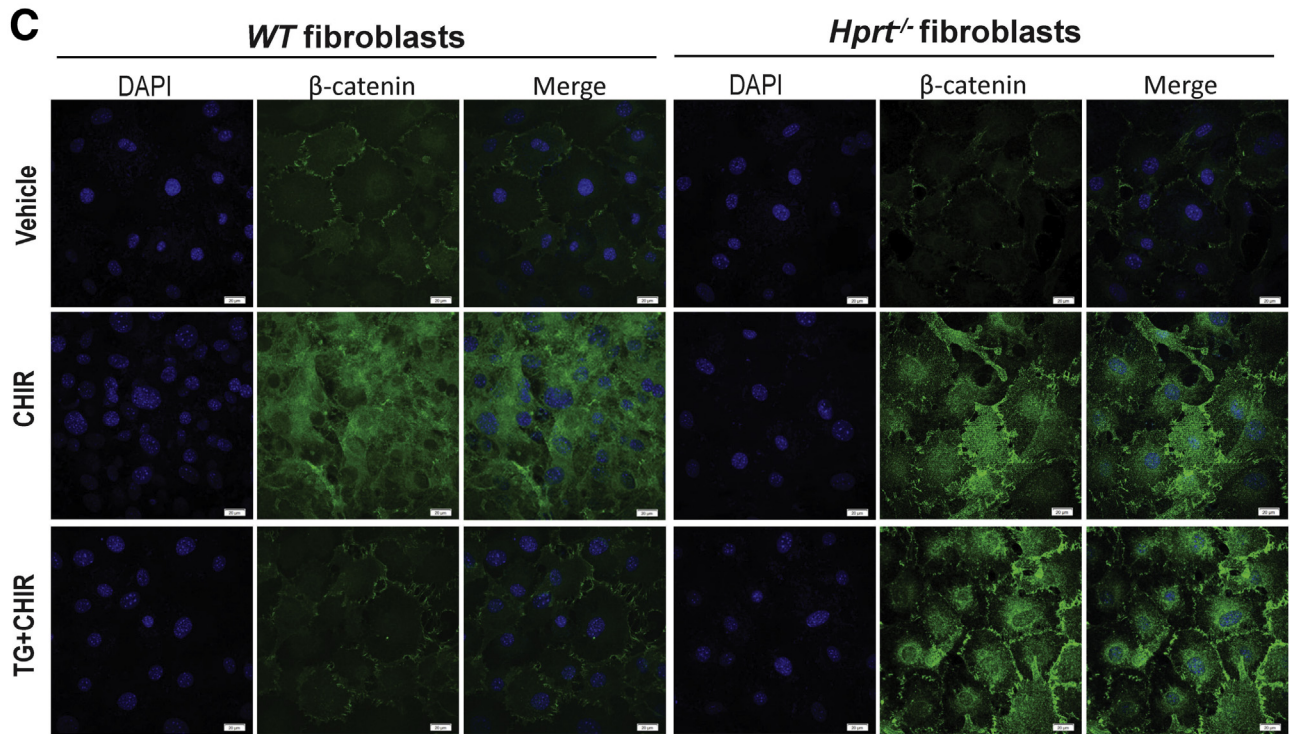
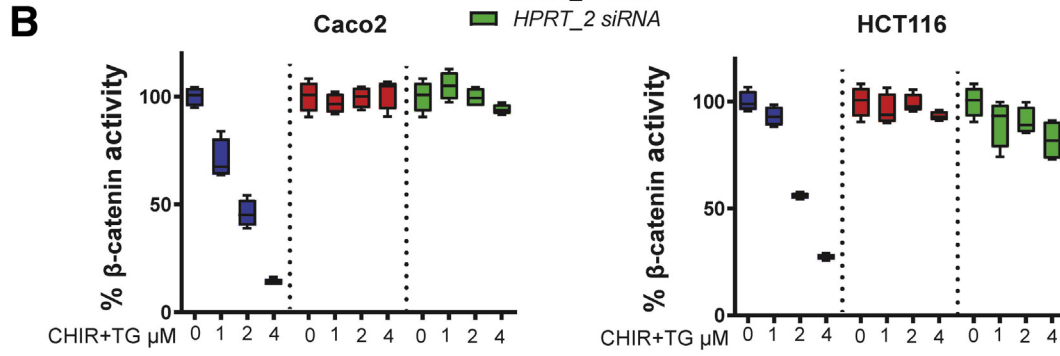
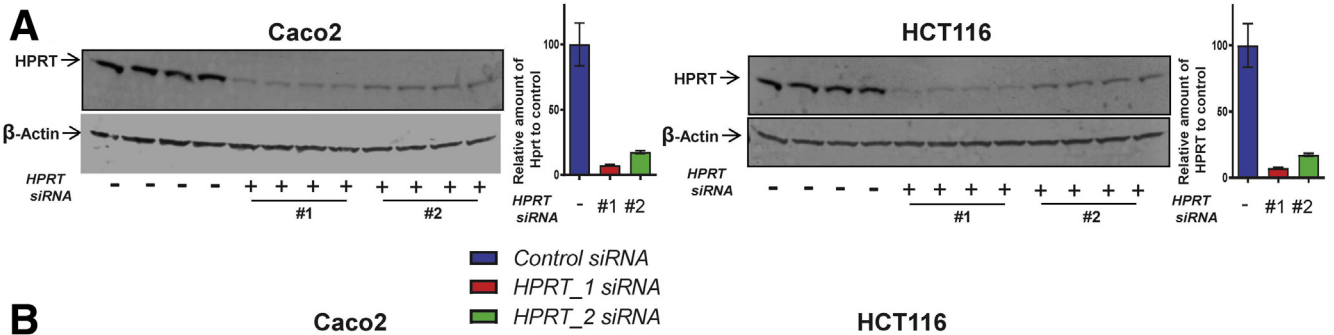


Figure 7. TG inhibits β -catenin activity in vitro independently of autophagy. (A) Knockdown of ATG7 in Caco2 and HCT116 cells 48 hours after transfection with ATG7 (#3) or ATG7 (#4) or control (-) siRNA was assessed by Western blotting. (B) Basal β -catenin-driven transcriptional activity in Caco2 and HCT116 cells transfected with ATG7 or control siRNA for 48 hours was increased with inhibition of the autophagy gene. (N = 4). (C) Treatment of the same cells in presence of 1 μ mol/L CHIR-99021 and indicated dose of TG for 16 hours inhibited β -catenin-driven transcriptional activity. Data are representative of 4 independent experiments. RLU, relative light units.

cytoplasmic and nuclear fractions of β -catenin on TG treatment in WT fibroblasts; the decrease was more marked, not unexpectedly, in the nuclear fractions from the CHIR-stimulated WT fibroblasts. As expected, TG was not associated with decreased cytoplasmic and nuclear fractions of β -catenin from *Hprt*^{-/-} fibroblasts (Figure 8D), thus confirming that TG's inhibition of β -catenin activity is mediated by TGN, most likely involving TGTP (Figure 1A).

Thioguanine Suppression of β -Catenin Activity Is Dependent on Rac1 at Lower Concentrations

TGN interact with Rac1, a Rho family GTPase that binds to guanosine triphosphate (GTP) in its active form, to inhibit proliferation of activated blood lymphocytes.^{24,25} To determine whether TGN also inhibit β -catenin activity in colonic epithelial cells via Rac1, we examined the effect of Rac1 silencing on β -catenin transcriptional activity in HCT116 and Caco2 cells using the luciferase reporter assay



(Figure 9A). The siRNA silencing of *Rac1* induced a decrease in β -catenin transcriptional activity in these cells. At the IC50 dose of TG (2 $\mu\text{mol/L}$), there was no additional inhibition of β -catenin transcriptional activity in the presence of *Rac1* silencing, indicating that at this dose, TG-mediated inhibition is *Rac1* dependent. However, a higher concentration of TG (20 $\mu\text{mol/L}$) did also inhibit β -catenin transcriptional activity (Figure 9B), indicating an additional *Rac1* independent effect of TG on β -catenin activity at a supraphysiological higher concentration.

To better define the role of *Rac1* mediated activation of β -catenin, we studied β -catenin activity in HCT116 and Caco-2 cells expressing mutant *Rac1*^{Q61L}, in which *Rac1* exists constitutively in the GTP-bound (activated) form. Normally, hydrolysis of bound GTP by *Rac1* GTPase to *Rac1*-guanosine diphosphate (GDP) results in its inactivation (Figure 9C.1). When TGTP binds *Rac1* and is hydrolyzed to TGDP, it cannot be exchanged for GTP or TGTP by guanosine exchange factor (Figure 9C.2),²⁵ leading to a decreased pool of *Rac1* that can be activated to *Rac1*-GTP. In cells expressing mutant *Rac1*^{Q61L}, we hypothesized that β -catenin activity would be constitutively up-regulated (Figure 9C.3) because of defective intrinsic GTPase activity and thus unresponsive to TG.

In WT cells transfected with vector only, β -catenin transcriptional activity was inhibited by TG in an expected dose-response fashion, but 1–4 $\mu\text{mol/L}$ TG was ineffective in *Rac1*^{Q61L} active mutant transfected cells. However, higher dose TG (>4 $\mu\text{mol/L}$) inhibited β -catenin transcriptional activity in *Rac1*-Q61L active mutant transfected cells (Figure 9D). Taken together with the siRNA results, these data indicate that suppression of β -catenin transcriptional activity via inhibition of activated *Rac1* occurs at concentrations of TG that correspond to the IC50, but that higher concentrations of TG inhibit β -catenin transcriptional activity via *Rac1*-independent mechanisms.⁴⁴ One possibility is that TGTP may directly inhibit β -catenin. To determine whether there is a potential binding site, molecular docking experiments were performed by using the crystal structure of the armadillo repeat region of human β -catenin.⁴⁵ In these modeling experiments, TGTP docked with β -catenin protein with a binding free energy ΔG value of -47.11 kcal/mol (Figure 9E). The docking of TGTP ligand in the conserved *Rac1* nucleotide binding site is shown in Figure 9E with corresponding ΔG value of -58.53 kcal/mol.

Discussion

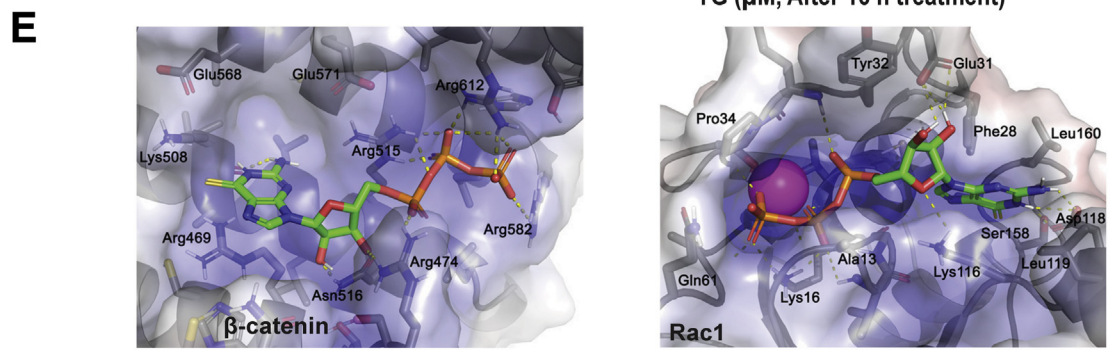
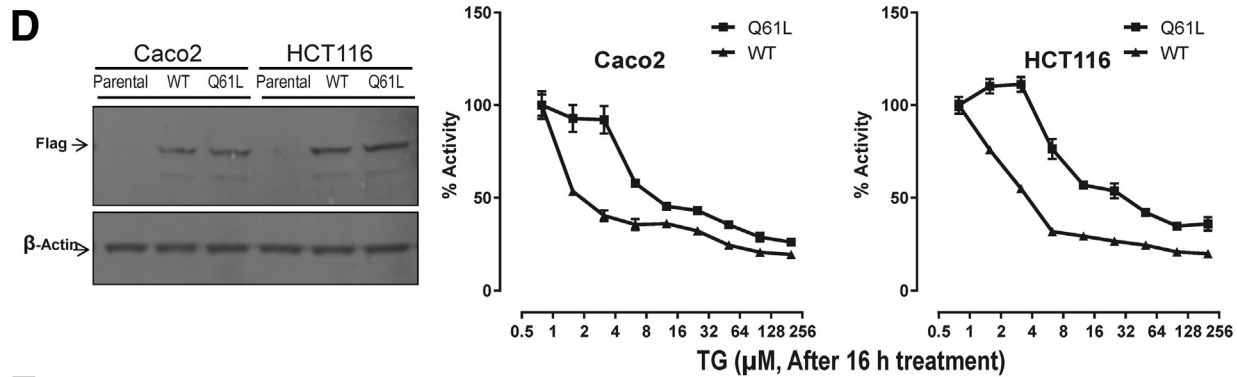
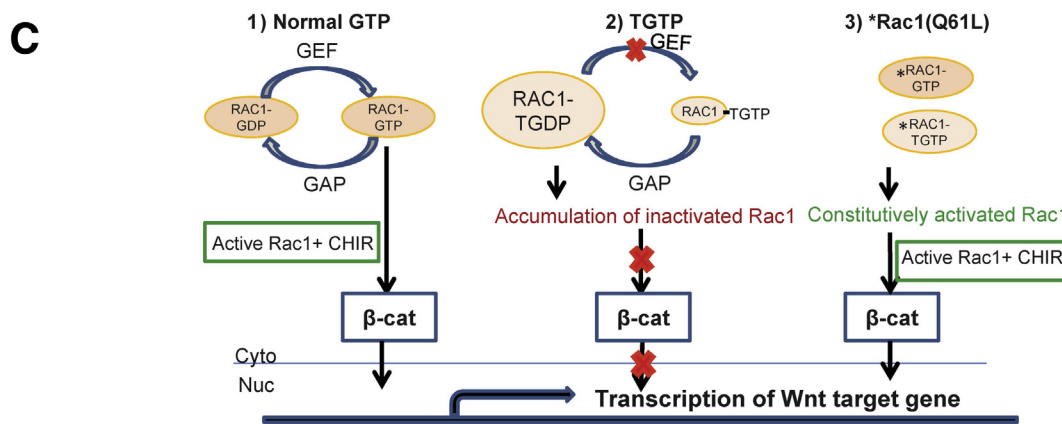
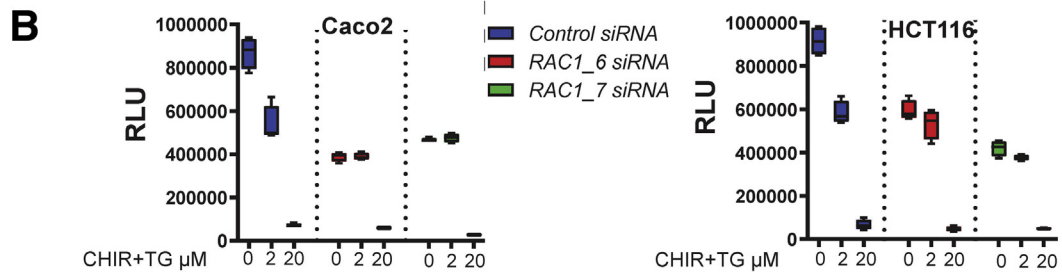
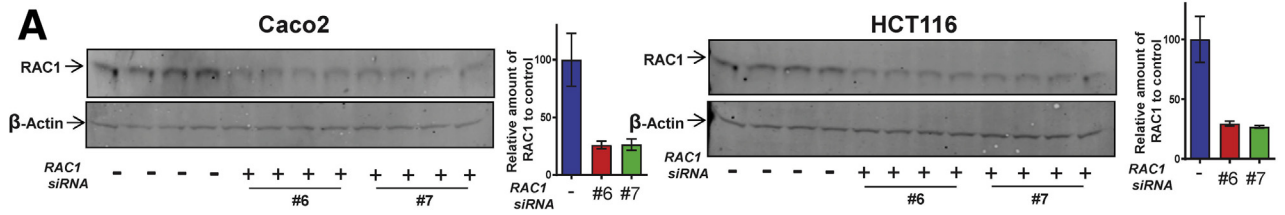
In this study, we provide evidence to indicate that TG but not MP acts directly on intestinal epithelial cells in vitro to inhibit β -catenin activity. This effect of TG was

also confirmed in ex vivo epithelial cells from N = 1 colon cancer, which was resected from a patient with ulcerative colitis (Figure 1D). The action on β -catenin activity is in addition to TG's known actions on immune cells. The inability of MP to inhibit β -catenin activity is likely related to its rate-limited conversion to TGN as well as other MP metabolites. We further demonstrate that daily intrarectal TG inhibits colonic tumorigenesis in vivo in a murine CAC model, that the mechanism of action to inhibit CAC is dependent on TG's conversion to TGN, that the mechanism is largely independent of TG's action on intestinal inflammation, which requires autophagy induction in intestinal epithelial cells, and that the antitumorigenic activity is via suppression of *Rac1*-mediated β -catenin nuclear translocation, which results in both reduced proliferation of colonic epithelial cells and transcription of oncogenic genes.

Our finding that TG but not MP effects a rapid inhibition of β -catenin activity advances current concepts about the mechanism of action of TG in the treatment of IBD and prevention of CAC. Unlike azathioprine and MP, the mechanism of rectal TG in abrogating colitis and preventing CAC involves a direct effect on epithelial cells. Conversion to TGN from MP and azathioprine⁴⁶ for their therapeutic effects is rate-limited by IMPDH and occurs mainly in liver and circulating leukocytes.³⁴ While systemic conversion of thiopurine pro-drugs to TGTP inhibits proliferation and promotes apoptosis of activated immune cells via *Rac1* to reduce overall inflammation, our data suggest that the effect of locally administered TG on colonic epithelium relies on rapid local conversion to TGN in the epithelium.

We found that the anti-inflammatory properties of topical TG were dependent on intact autophagy machinery, which is consistent with a TG-mediated up-regulation of autophagy leading to decreased colitis. This is significant because the common ATG16L1T300A polymorphism is associated with decreased autophagy and a higher risk of developing IBD.⁴⁷ Because there was a >50% reduction of tumor burden in animals with disrupted autophagy machinery in the epithelial cell compartment (Figure 3), the largely autophagy-independent mechanism of action to prevent CAC is entirely consistent with (i) the demonstrated mechanism of action via inhibition of β -catenin, which occurs despite a role for autophagy in the development of CRC,³⁰ (ii) reports that disruption of *Atg7* in a model of sporadic CRC (*APC*^{min}) decreases tumor initiation,³² and (iii) evidence that TG's anti-inflammatory effect in epithelial cells involves autophagy.³⁶ As in previous studies of tissue-specific ATG7 disruption in intestinal epithelial cells,³² our

Figure 8. (See previous page). TG inhibits β -catenin activity via TGN. (A) Knockdown of *HPRT* in Caco2 and HCT116 cells 48 hours after transfection with *HPRT* (#1) or *HPRT* (#2) or control (-) siRNA, assessed by Western blotting. (B) TG in presence of 1 $\mu\text{mol/L}$ CHIR-99021 versus β -catenin-driven transcriptional activity in cells silenced with *HPRT* siRNA. (C) WT and *Hprt*^{-/-} derived primary murine fibroblasts treated with 5 $\mu\text{mol/L}$ CHIR \pm 10 $\mu\text{mol/L}$ TG or vehicle for 16 hours. Immunofluorescence staining for β -catenin (green) and nuclei (DAPI, blue). Data are representative of 4 independent experiments. (D) Western blotting of cytosol and nuclear compartments of WT and *Hprt*^{-/-} derived primary murine fibroblasts treated with 5 $\mu\text{mol/L}$ CHIR \pm 10 $\mu\text{mol/L}$ TG or vehicle for 16 hours showing TG inhibiting β -catenin activity and nuclear translocation with CHIR only in WT cells.



data (Figure 3) demonstrate a lower rate of tumor initiation and growth in the absence of autophagy.

In addition to the mechanism of prevention of colon tumorigenesis by TG elucidated in the present study, the magnitude of the effect was strikingly large, compared with the magnitude of the cancer chemopreventive effect of azathioprine and MP reported in large epidemiologic studies.^{22,23,48,49} The current paradigm is that their onco-protective property relates to their anti-inflammatory effect, although not all studies confirm the effect.⁵⁰ Similarly, it has been proposed that targeting of the interleukin 23 pathway should prevent CAC in IBD by treating inflammation.²⁸ Also consistent with this paradigm, there are large epidemiologic studies that report a cancer chemoprophylaxis effect with mesalamine in ulcerative colitis,⁵¹ although this is also contested.⁵²

An alternative possibility for the reported cancer-chemoprophylactic benefit of azathioprine and MP is that their beneficial action is mediated by a similar mechanism of action as the present study demonstrates for intrarectal TG, ie, by RAC1-mediated inhibition of β -catenin activity in epithelial cells. However, although azathioprine and MP are converted in vivo via IMPDH and HPRT to TGN in circulating blood cells, it is difficult to envisage how TGN might exchange into intestinal epithelial cells from circulating red and white blood cells because the TGN are intracellular, and TGN do not exist extracellularly.

Constitutive nuclear β -catenin expression and over-activated Wnt/ β -catenin signalling have been reported in several cancers, including CRC, where they promote growth, invasion, and metastasis in cancer.^{53,54} Although systemic conversion of thiopurine pro-drugs to TGTP inhibits proliferation and promotes apoptosis of activated immune cells via Rac1 to so reduce overall inflammation, we show that the effect of locally administered TG on colonic epithelium requires local conversion to TGN to inhibit Wnt/ β -catenin signalling. Rac1, which binds to TGTP, mediated the action of low-dose TG on β -catenin activity in colon cancer cell lines, but there were other actions with higher doses of TG in the colon cancer cell lines such as might occur with binding of TGTP to β -catenin (Figure 9E) or other mechanisms. In summary, the novel findings regarding the potency and pharmacologic mechanism of action of TG in epithelial cells add to our understanding of the biology of colon cancer prevention in the setting of chronic colonic inflammation and suggest that local administration of TG may independently reduce the risk of CAC through a novel mechanism involving RAC1 GTPase and canonical β -catenin signalling.

Materials and Methods

Cell Culture, Transfection, and Infection

Human HCT116 and Caco2 intestinal epithelial cells were obtained from the American Type Culture Collection (Rockville, MD) and propagated in Dulbecco modified Eagle medium (DMEM) (Life technologies, Carlsbad, CA) with 10% heat inactivated fetal calf serum, 100 U mL⁻¹ penicillin, 100 μ g mL⁻¹ streptomycin, and 2 mmol/L L-glutamine. All these cell lines were authenticated by short tandem repeat profiling, were mycoplasma-free, and underwent 5 or fewer passages.

Signal Lenti T-Cell Factor/Lymphoid Enhancer Factor Reporter Luciferase Assay

Signal Lenti transcriptional response element reporter lentivirus particles, which express a luciferase gene driven by multiple TCF/LEF (AGATCAAAGGGGTA) repeats and Signal Lenti Renilla control lentivirus particles, were purchased from QIAGEN (Hilden, Germany) (#CLS-018L). HCT116 and Caco2 cells were transduced with TCF/LEF promoter along with Renilla luciferase (selected with puromycin). Stable HCT116 and Caco2 pooled clones over-expressing reporter construct were treated with 1 μ mol/L CHIR 99021 (Selleckchem, Houston, TX) for 16 hours. Luciferase activity was measured on Titertek Berthold luminometer by using the Dual Luciferase reporter assay (Promega, Madison, WI) according to the manufacturer's protocol.

Immunofluorescence

For immunofluorescence, cells were seeded on coverslips in 24-well plates and fixed with 4% paraformaldehyde for 20 minutes at ambient temperature. After 3 phosphate-buffered saline with 0.1% Tween-20 (PBS-T) washes, cells were blocked with 5% bovine serum albumin (BSA) in PBS-T for 30 minutes at 37°C and then blocked with the Image-It @FX Signal Enhancer Ready Probes Reagent (Life Technologies, Carlsbad, CA) 30 minutes at 37°C. Cells were incubated with the anti- β -catenin (#8480, clone D10A8; Cell Signaling Technology, Danvers, MA) in PBS-T with 1% BSA overnight at 4°C. After 3 washes (10 minutes each), the slides were incubated with Alexa Fluor 594 goat anti-rabbit (Molecular Probes, Eugene, OR) prepared in PBS-T with 2% BSA. The slides were counterstained with DAPI (Molecular Probes) and imaged by using the confocal laser-scanning microscope Olympus FV1200 (Tokyo, Japan) microscopy.

Figure 9. (See previous page). TG at low concentrations suppressed β -catenin activation via inhibition of Rac1. (A) Knockdown of Rac1 in Caco2 and HCT116 cells 48 hours after transfection with *Rac1* siRNA #6 or *Rac1* siRNA #7 versus control (-) siRNA, assessed by Western blotting. (B) [TG] versus β -catenin-driven transcriptional activity in control cells versus *Rac1*-siRNA silenced cells. (C) Cartoon showing role of Rac1 in β -catenin-driven transcription of Wnt target gene: C1, normal physiology with GTP; C2, TG with WT Rac1; C3, TG with genetically inactivated GTPase Q61L Rac1. (D) *Left panel*: Western blotting for Flag in HCT116 and Caco2 cells confirms overexpression of Rac1 WT and Rac1 mutant in these cells. *Right panels*: [TG] versus β -catenin-driven transcriptional activity in WT and Q61L (ie, constitutively active Rac1). Caco2 and HCT116 cells. Data are representative of 3 independent experiments. (E) Modelling experiments showing TGTP docked with β -catenin protein crystal structure (*left panel*) and docked in the conserved Rac1 nucleotide binding site (*right panel*). RLU, relative light units.

Spheroids

Ulcerative colitis-associated CRC specimen used in this study was collected with written informed consent from one patient undergoing surgical resection under the approval of the Mater Research Ethics Committee. Tumor tissue freshly resected from the patient was dissociated into single cells and grown as a suspension culture in a serum-free medium that consisted of Advanced DMEM/F12 medium (Thermo Scientific, Mulgrave, Australia), 0.4% BSA (Sigma, Castle Hill, Australia), 5 mmol/L HEPES (Thermo Scientific), 1× GlutaMax (Thermo Scientific), 4 μg/mL heparin (Sigma), 0.3% D-glucose (Sigma), 1% B27 supplement without vitamin A (Thermo Scientific), 1% N2 supplement (Thermo Scientific), 10 μg/mL insulin (Sigma), 1 mmol/L N-acetyl-L-cysteine (Sigma), 10 mmol/L nicotinamide (Sigma), 20 ng/mL EGF (Thermo Scientific), and 20 ng/mL FGF (R&D Systems, Minneapolis, MN) for 14 days in low-adhesion plates (Corning, Tewksbury, MA) at a density of 1×10^5 cells per mL. These conditions select for cells with the capacity to grow as spheroids that display stemness properties including the ability to reinitiate tumor growth in vivo.⁵⁵ The established spheres were treated with 10 μmol/L TG or vehicle control for 4 days, and then spheres were harvested by centrifugation at 30g for 4 minutes, washed twice with PBS, and fixed in 4% paraformaldehyde in PBS for 20 minutes. Fixed spheres were permeabilized with 0.2% Triton X-100 in PBS for 10 minutes, washed 3 times with PBS, and then residual aldehyde quenched by addition of ammonium chloride (50 mmol/L) for 10 minutes. Nonspecific binding sites on PBS washed spheres were blocked with 0.2% albumin in PBS for 30 minutes. Spheres were incubated overnight in blocking buffer containing rabbit anti-active β-catenin antibody D13A1 (1:100; Cell Signaling #8814) and mouse anti-β-catenin (1:100; BD #610154; San Jose, CA) antibodies. After 3 washes with PBS, spheres were incubated for 30 minutes in blocking buffer containing 46-diamidino-2-phenylindole (DAPI) and fluorescently tagged secondary antibodies. Fluorescent signals from spheres were acquired by using an Olympus FV1200 microscope confocal microscope.

Immunoblot Analysis

Protein concentrations were measured by using the BCA Protein Assay Kit (Thermo Scientific, Waltham, MA) with BSA as a standard. Aliquots of the lysate containing 30 μg total protein were mixed in sodium dodecyl sulfate–polyacrylamide gel electrophoresis Laemmli buffer (0.05 mol/L Tris-HCl, pH 6.8, 0.1% 2-mercaptoethanol, 1.0% sodium dodecyl sulfate, 5% glycerol, and 0.15% bromophenol blue), boiled for 5 minutes, and resolved on 4%–12% acrylamide gels. Resolved proteins were transferred to polyvinylidene difluoride membranes for Western blotting, probed with appropriate antibodies at the manufacturer recommended dilutions, and detected by dual-label infrared analysis, imaged on Odyssey XL scanning system (LI-COR BIOSCIENCES, Lincoln, NE), and analysis on Image Studio software version 5.2 (LI-COR BIOSCIENCES).

Atg7^{ΔIEC} C57Bl/6 Mice

Atg7 is an autophagy gene whose expression is essential for the biogenesis of autophagosomes³¹; homozygous loss of *Atg7* is lethal at birth.⁵⁶ Therefore, for these experiments we used conditional targeting of the *Atg7* locus (*Atg7*^{f/f}), bred with villin-Cre-expressing mice to enable analysis of epithelial cell specific functions of *Atg7*^{ΔIEC} (*Atg7*^{f/f} × villin-Cre) mice and its littermates, henceforth referred to as *Atg7*^{ΔIEC} and *Atg7*^{+/+} mice, respectively.

Tumor Induction

Colon tumors were induced by AOM and DSS model. Briefly, 4- to 5-week-old WT or *Atg7*^{ΔIEC} C57Bl/6 mice were injected intraperitoneally with 10 mg AOM (A5486; Sigma-Aldrich, St Louis, MO) per kg body weight. Seven days later, 1.5% DSS (molecular mass 36–40 kDa) was given in the drinking water for 5 days, followed by regular drinking water for 2 weeks, and the DSS cycle was repeated twice. TG-treated and vehicle-treated mice were housed separately. Symptoms of colitis were assessed by the DAI.⁵⁷ The DAI is a score based on sum of subscores for diarrhea, rectal bleeding, and loss of body weight. Mice were killed on day 85, and the person dissecting the colons was blinded to the treatment. Colon tissues were fixed in 10% formalin, embedded in paraffin, sectioned, and stained with H&E. The number of proliferating cells in the intestinal epithelium was detected by BrdU as described below and previously.⁵⁷

β-Catenin Immunohistochemistry Staining and Histology Image Analysis

Sections from paraffin-embedded tissues or tumors were deparaffinized, rehydrated, and antigen-retrieved by heating for 20 minutes in 10 mmol/L citric acid (pH 6), cooled to room temperature, and then treated with 3% hydrogen peroxide in PBS for 10 minutes. Sections were then stained with the anti-β-catenin antibody (#8480, clone D10A8; Cell Signaling Technology) at 1/200 dilution and detected with anti-rabbit antibody-horseradish peroxidase (BD Pharmingen) and DAB. Histology sections stained with β-catenin were analyzed by using Visiopharm software version 2017.2 (Hoersholm, Denmark). The software allowed for quantification of specific tissue areas and measurement of percentage of positive cells and intensity (0–255) of the staining in these areas.

Growth Curves Assay

Cells (7500 cells/well) were plated in a 96-well plate and visualized by using a real-time cell imaging VL21 system (Phase Focus Limited, Sheffield, UK), which uses a method known as ptychography in image formation. Growth curves were built from confluence measurements acquired during round-the-clock kinetic imaging.

Proliferation Assays

To assess proliferation in vivo, mice were given 100 μg/g body weight of BrdU intraperitoneally 1.5 hours before euthanasia for tissue or tumor sampling. Paraffin sections

were processed, and antigen was retrieved as detailed above. Sections were then stained with the biotinylated anti-BrdU antibody (#ab6326, clone ICR1; Abcam, Cambridge, UK) at 1/100 dilution and detected with streptavidin-horseradish peroxidase (BD Pharmingen) and DAB.

Reagents and Antibodies

All reagents and chemicals were purchased from Sigma-Aldrich unless otherwise stated. AOM (A5486; Sigma-Aldrich, DSS; molecular mass 40–50 kDa) was purchased from Affymetrix (Santa Clara, CA). Complete protease inhibitor cocktail and phosphate stop were purchased from Roche (Basel, Switzerland). CHIR 99021(CHIR) was purchased from Selleckchem (Houston, TX).

The antibodies used in this study were anti- β -catenin (#8480, clone D10A8; Cell Signaling Technology), anti-Non-Phospho- β -catenin (#19807, clone D2U8Y; Cell Signaling Technology), anti-Cyclin D1 (#2978, clone 92G2; Cell Signaling Technology), anti-C-Jun (#9165, clone 60A8; Cell Signaling Technology), anti-CD44 (#3570; Cell Signaling Technology), anti-MMP7 (#3801, clone D4H5; Cell Signaling Technology), anti-Survivin (#2808, clone 71G4B7; Cell Signaling Technology), anti-ATG7 (#MAB6608, clone 683906; R&D Systems), anti- β -actin (#MAB1501; Novus Biologicals, Littleton, CO), anti-HPRT (#ab16048; Abcam), anti-Rac1 (#05-389, clone 23A8; Millipore, Burlington, MA), and anti-lamin B (#ab16048; Abcam).

Disease Activity Index Scores

The DAI scores are defined as the sum of subscores for diarrhea, rectal bleeding, and loss of body weight. Diarrhea scores ranged from 0 to 3, with 0 being none and 3 being frank diarrhea; rectal bleeding ranged from 0 to 3, with 0 being no bleeding and 3 being frank rectal bleeding. Body weight percent loss subscores were 0 = <5% loss; 1 = 5%–15% loss; 2 = 15%–20% loss; and 3 >20% loss.

Small Interfering RNAs

Small interfering RNAs targeting *ATG7* (FlexiTube GeneSolution GS10533 for *ATG7*, catalog #1027416), *HPRT* (FlexiTube GeneSolution GS3251 for *HPRT1*, catalog #1027416), and *RAC1* (FlexiTube GeneSolution GS5879 for *RAC1*, catalog #1027416), and non-targeted control siRNA (Negative Control siRNA negative (non-silencing) control siRNA, catalog #SI03650325) were purchased from QIAGEN. Oligonucleotide transfection was performed with Lipofectamine 2000 Reagent (Life Technologies) at a final concentration of 50 nmol/L, and cells were harvested for the assays 48 hours after transfection.

Generation of Stable *Rac1* Wild-type and Mutant *Rac1*^{Q61L} Cell Lines

WT or activated mutant *Rac1*^{Q61L} flag-tagged constructs in pcDNA3.1 were from GenScript (Piscataway, NJ). DNA fragments encoding *RAC1* WT or activated mutant *Rac1*^{Q61L} flag-tagged were then cloned into a Lentiviral construct pLenti CMV Hygro DEST vector (Addgene, Cambridge, MA)

using Gateway LR recombination cloning technology (Life Technologies) (Figure 9D). For stable cell lines, 5×10^6 amphotropic (HEK293) packaging cells were transfected with 10 μ g DNA of the appropriate construct by Lipofectamine 2000 Reagent according to the manufacturer's protocol. Culture supernatants were collected 36–48 hours after transfection and filtered through 0.45 μ m filter. HCT116 and Caco2 cells were infected with the filtered viral supernatants in the presence of 4 μ g/mL polybrene (Sigma-Aldrich) for 12 hours, after which the medium was changed. Fresh viral suspensions were added after a 24-hour interval for an additional 12 hours. Infected cells were selected for 5 days in 200 μ g mL⁻¹ hygromycin.

Measurement of Thioguanine Nucleotides

HCT116 or Caco2 colon cells (25,000 cells/well) were cultured for 16 hours in 96-well plates with TG or MP or vehicle control substrate. TGN were measured in the washed colon cells by the Queensland Pathology Service's laboratory using an automated modified Dervieux and Bouliou method⁵⁸ with liquid chromatography–mass spectrometry detection. The limit of quantification for measuring TGN in our cultures without an additional concentration step was 0.5 μ mol/L.

Instrumentation and reagents. An Acquity UPLC system with a binary solvent manager, sample manager, QDa single quadrupole mass detector, and Empower 3 Chromatography data manager were used. An Atlantis T3 C18 column (3.0 μ m particles; 2.1 \times 100 mm) was used to optimize the chromatographic conditions. The equipment and reagents mentioned above were sourced from Waters Corporation (Milford, MA). Formic acid (Sigma-Aldrich) and acetonitrile (Thermo Fisher) were MS-grade.

Sample preparation. We mixed 200 μ L sample, 100 μ L Internal Standards (6TG-¹³C2 ¹⁵N), 100 μ L dithiothreitol, and 100 μ L 35% perchloric acid in 1-mL-deep 96-well plate on Biosan Laboratories (Warren, MI) 96-well heater/mixer at 100°C for 60 minutes. The 96-well plate was centrifuged and placed into the sample manager.

Optimized chromatography and mass spectrometry conditions. The column temperature was 45°C, flow rate of 0.4 mL/min, with the initial conditions of 99% mobile phase A (0.1% formic acid in water) and 1% mobile phase B (0.1% formic acid in acetonitrile). After 1 μ L sample is injected, a linear gradient (curve 6) is applied to 97% A at 1 minute, followed by 80% A at 2 minutes, and 1% A at 2.1 minutes before returning to initial conditions at 2.50 minutes. The MS detector was programmed to collect single ion reactions of selected atomic masses in positive ionization mode during the expected time interval (6TG, 167.93 Da and 6TG IS, 170.92 Da). The probe temperature was 600°C, the capillary voltage was 0.8 kV, cone voltage was 5V, and the sampling rate was 5 points/second.

Cell Viability WST-1 Colorimetric Assay

WST-1 (4-(3-(4-iodophenyl)-2-(4-nitrophenyl)-2H-5-tetrazolio)-1,3-benzene disulfonate; cat. no. 11644807001; Roche Applied Science) colorimetric assay was carried out

to determine the effects of 16 hours of TG treatment on cell viability. The stable tetrazolium salt WST-1 is cleaved to a soluble formazan by a complex cellular mechanism that occurs primarily at the cell surface. This bioreduction is largely dependent on the glycolytic production of reduced nicotinamide adenine dinucleotide phosphate in viable cells. Therefore, the amount of formazan dye formed directly correlates to the number of metabolically active cells in the culture. The assay was performed in 96-well plates, with seeding of ~25,000 cells in each well. After 16 hours of TG treatment, 20 μ L of the WST-1 solution was added to the culture medium and incubated for 2.5 hours at 37 °C. Absorbance was subsequently determined by using a microplate enzyme-linked immunosorbent assay reader (VERSAmax; Molecular Devices, Sunnyvale, CA) and analyzed with SoftMax Pro 5 Software (Molecular Devices) by applying the wavelengths 450 nm for measurements and 650 nm as reference. All experiments were conducted in 4 wells for each condition and replicated at least 3 times.

Molecular Docking

Crystal structures of β -catenin (1G3J.pdb) and Rac1 (1MH1.pdb) were retrieved from the RSCB Protein Data Bank⁵⁹ and prepared for modelling by using the Protein Preparation Wizard in Schrödinger Release 2019-2 software (New York, NY). The crystal structures were assigned bond orders, hydrogens were added, and protonation states of ionizable groups were assigned at pH = 7.4 \pm 1.0 with Epik. The OPLS3e force field⁶⁰ was used to minimize protein hydrogen atoms with restraints on heavy atoms. In preparation for docking experiments all solvent molecules were removed from the binding sites. Ligand structures were retrieved from the PubChem database and prepared for docking by using LigPrep. LigPrep assigned bond orders, stereochemistry, added hydrogens, and set protonation states of ionizable groups at pH = 7.4 \pm 1.0 using Epik. Final ligand structures were minimized with the OPLS3e force field ready for docking.

Docking experiments were performed by using the Schrödinger Suite Glide module. A Glide docking grid of β -catenin was prepared by using default parameters and centered on Arg469. Similarly, a Glide docking grid was prepared for Rac1 by using default parameters centered on the co-crystallized ligand guanosine-5'-(beta gamma-imino) triphosphate (GMPPNP). The docking grid for Rac1 also included interaction constraints to the Mg⁺ ion and a core atom constraint applied to the 6-membered ring of the purine group. Glide standard precision docking with default parameters was used to dock TMGP into the binding site of β -catenin with the top 10 docked conformers kept. Similarly, Glide standard precision was used to dock ligands TMGP and GMPPNP into the binding site of Rac1. Docked conformations were constrained with a core constraint to the 6-membered ring of the purine group, and the ligand had to interact with the Mg⁺ ion. The top 3 docked poses of TGTP in β -catenin were submitted to a Prime MMGBSA calculation to determine a calculated Δ G of binding. Prime MMGBSA calculations included the docked ligand and

sidechain atoms of residues within 6 Å of the ligand. Prime used the OPLS3e force field with the updated solvent model VSGB2.1⁶¹ to perform all optimizations and calculations. Similarly, crystal pose of GMPPNP and the top Glide docked poses of TGTP and GMPPNP were submitted to a Prime-MMGBSA calculation to determine their calculated Prime MMGBSA Δ G of binding.

Ethics

All experiments were approved by the University of Queensland Animal Ethics Committee.

All authors had access to the study data and reviewed and approved the final manuscript.

Statistical Analysis

All statistical analyses were performed by using Prism v5 (Graphpad Software, San Diego, CA). Sample sizes for experiments were determined by power analyses based on the variation shown in previous experiments and predicted effect sizes considered to be of biological relevance. No data were excluded from any analyses. The normal distribution of data was assessed by probability plots, and where a normal distribution could not be established, nonparametric testing was used. The statistical test used and the sample sizes for individual analyses are provided within the figure legends.

References

1. Ng SC, Shi HY, Hamidi N, Underwood FE, Tang W, Benchimol EI, Panaccione R, Ghosh S, Wu JCY, Chan FKL, Sung JY, Kaplan GG. Worldwide incidence and prevalence of inflammatory bowel disease in the 21st century: a systematic review of population-based studies. *Lancet* 2018;390:2769–2778.
2. Terzić J, Grivennikov S, Karin E, Karin M. Inflammation and colon cancer. *Gastroenterology* 2010; 138:2101–2114 e5.
3. Qu D, Shen L, Liu S, Li H, Ma Y, Zhang R, Wu K, Yao L, Li J, Zhang J. Chronic inflammation confers to the metabolic reprogramming associated with tumorigenesis of colorectal cancer. *Cancer Biol Ther* 2017;18:237–244.
4. Ferlay J, Colombet M, Soerjomataram I, Mathers C, Parkin DM, Pineros M, Znaor A, Bray F. Estimating the global cancer incidence and mortality in 2018: GLOBOCAN sources and methods. *Int J Cancer* 2019; 144:1941–1953.
5. Bray F, Ferlay J, Soerjomataram I, Siegel RL, Torre LA, Jemal A. Global cancer statistics 2018: GLOBOCAN estimates of incidence and mortality worldwide for 36 cancers in 185 countries. *CA Cancer J Clin* 2018; 68:394–424.
6. Shen P, Pichler M, Chen M, Calin GA, Ling H. To Wnt or lose: the missing non-coding linc in colorectal cancer. *Int J Mol Sci* 2017;18.
7. Najdi R, Holcombe RF, Waterman ML. Wnt signaling and colon carcinogenesis: beyond APC. *J Carcinog* 2011; 10:5.

8. Clevers H. Wnt/beta-catenin signaling in development and disease. *Cell* 2006;127:469–480.
9. Spranger S, Gajewski TF. Tumor-intrinsic oncogene pathways mediating immune avoidance. *Oncoimmunology* 2016;5:e1086862.
10. Hong Y, Manoharan I, Suryawanshi A, Majumdar T, Angus-Hill ML, Koni PA, Manicassamy B, Mellor AL, Munn DH, Manicassamy S. Beta-catenin promotes regulatory T-cell responses in tumors by inducing vitamin A metabolism in dendritic cells. *Cancer Res* 2015;75:656–665.
11. Augustin I, Dewi DL, Hundshammer J, Rempel E, Brunk F, Boutros M. Immune cell recruitment in teratomas is impaired by increased Wnt secretion. *Stem Cell Res* 2016;17:607–615.
12. Cooper HS, Murthy S, Kido K, Yoshitake H, Flanigan A. Dysplasia and cancer in the dextran sulfate sodium mouse colitis model: relevance to colitis-associated neoplasia in the human—a study of histopathology, B-catenin and p53 expression and the role of inflammation. *Carcinogenesis* 2000;21:757–768.
13. Aust DE, Terdiman JP, Willenbacher RF, Chang CG, Molinaro-Clark A, Baretton GB, Loehrs U, Waldman FM. The APC/beta-catenin pathway in ulcerative colitis-related colorectal carcinomas: a mutational analysis. *Cancer* 2002;94:1421–1427.
14. Claessen MM, Schipper ME, Oldenburg B, Siersema PD, Offerhaus GJ, Vleggaar FP. WNT-pathway activation in IBD-associated colorectal carcinogenesis: potential biomarkers for colonic surveillance. *Cell Oncol* 2010;32:303–310.
15. van Dekken H, Wink JC, Vissers KJ, Franken PF, Ruud Schouten W, WC JH, Kuipers EJ, Fodde R, Janneke van der Woude C. Wnt pathway-related gene expression during malignant progression in ulcerative colitis. *Acta Histochem* 2007;109:266–272.
16. Fearon ER. Molecular genetics of colorectal cancer. *Annu Rev Pathol* 2011;6:479–507.
17. Nusse R, Clevers H. Wnt/beta-catenin signaling, disease, and emerging therapeutic modalities. *Cell* 2017;169:985–999.
18. White BD, Chien AJ, Dawson DW. Dysregulation of Wnt/beta-catenin signaling in gastrointestinal cancers. *Gastroenterology* 2012;142:219–232.
19. Wu X, Tu X, Joeng KS, Hilton MJ, Williams DA, Long F. Rac1 activation controls nuclear localization of beta-catenin during canonical Wnt signaling. *Cell* 2008;133:340–353.
20. Esufali S, Bapat B. Cross-talk between Rac1 GTPase and dysregulated Wnt signaling pathway leads to cellular redistribution of beta-catenin and TCF/LEF-mediated transcriptional activation. *Oncogene* 2004;23:8260–8271.
21. Jess T, Lopez A, Andersson M, Beaugerie L, Peyrin-Biroulet L. Thiopurines and risk of colorectal neoplasia in patients with inflammatory bowel disease: a meta-analysis. *Clin Gastroenterol Hepatol* 2014;12:1793–1800 e1.
22. van Schaik FD, van Oijen MG, Smeets HM, van der Heijden GJ, Siersema PD, Oldenburg B. Thiopurines prevent advanced colorectal neoplasia in patients with inflammatory bowel disease. *Gut* 2012;61:235–240.
23. Beaugerie L, Svrcek M, Seksik P, Bouvier AM, Simon T, Allez M, Brixi H, Gornet JM, Altwegg R, Beau P, Duclos B, Bourreille A, Faivre J, Peyrin-Biroulet L, Flejou JF, Carrat F, Group CS. Risk of colorectal high-grade dysplasia and cancer in a prospective observational cohort of patients with inflammatory bowel disease. *Gastroenterology* 2013;145:166–175 e8.
24. Tiede I, Fritz G, Strand S, Poppe D, Dvorsky R, Strand D, Lehr HA, Wirtz S, Becker C, Atreya R, Mudter J, Hildner K, Bartsch B, Holtmann M, Blumberg R, Walczak H, Iven H, Galle PR, Ahmadian MR, Neurath MF. CD28-dependent Rac1 activation is the molecular target of azathioprine in primary human CD4+ T lymphocytes. *J Clin Invest* 2003;111:1133–1145.
25. Poppe D, Tiede I, Fritz G, Becker C, Bartsch B, Wirtz S, Strand D, Tanaka S, Galle PR, Bustelo XR, Neurath MF. Azathioprine suppresses ezrin-radixin-moesin-dependent T cell-APC conjugation through inhibition of Vav guanosine exchange activity on Rac proteins. *J Immunol* 2006;176:640–651.
26. Hofmann U, Heinkele G, Angelberger S, Schaeffeler E, Lichtenberger C, Jaeger S, Reinisch W, Schwab M. Simultaneous quantification of eleven thiopurine nucleotides by liquid chromatography-tandem mass spectrometry. *Anal Chem* 2012;84:1294–1301.
27. Seinen ML, van Nieuw Amerongen GP, de Boer NK, van Bodegraven AA. Rac attack: modulation of the small GTPase Rac in inflammatory bowel disease and thiopurine therapy. *Mol Diagn Ther* 2016;20:551–557.
28. Neurath MF. IL-23 in inflammatory bowel diseases and colon cancer. *Cytokine Growth Factor Rev* 2019;45:1–8.
29. Khor B, Gardet A, Xavier RJ. Genetics and pathogenesis of inflammatory bowel disease. *Nature* 2011;474:307–317.
30. Wu Y, Yao J, Xie J, Liu Z, Zhou Y, Pan H, Han W. The role of autophagy in colitis-associated colorectal cancer. *Signal Transduct Target Ther* 2018;3:31.
31. Komatsu M, Waguri S, Ueno T, Iwata J, Murata S, Tanida I, Ezaki J, Mizushima N, Ohsumi Y, Uchiyama Y, Kominami E, Tanaka K, Chiba T. Impairment of starvation-induced and constitutive autophagy in Atg7-deficient mice. *J Cell Biol* 2005;169:425–434.
32. Levy J, Cacheux W, Bara MA, L’Hermitte A, Lepage P, Fraudeau M, Trentesaux C, Lemarchand J, Durand A, Crain AM, Marchiol C, Renault G, Dumont F, Letourneur F, Delacre M, Schmitt A, Terris B, Perret C, Chamailard M, Couty JP, Romagnolo B. Intestinal inhibition of Atg7 prevents tumour initiation through a microbiome-influenced immune response and suppresses tumour growth. *Nat Cell Biol* 2015;17:1062–1073.
33. Ring DB, Johnson KW, Henriksen EJ, Nuss JM, Goff D, Kinnick TR, Ma ST, Reeder JW, Samuels I, Slabiak T, Wagman AS, Hammond ME, Harrison SD. Selective glycogen synthase kinase 3 inhibitors potentiate insulin activation of glucose transport and utilization in vitro and in vivo. *Diabetes* 2003;52:588–595.

34. Duley JA, Florin TH. Thiopurine therapies: problems, complexities, and progress with monitoring thioguanine nucleotides. *Ther Drug Monit* 2005;27:647–654.
35. De Robertis M, Massi E, Poeta ML, Carotti S, Morini S, Cecchetelli L, Signori E, Fazio VM. The AOM/DSS murine model for the study of colon carcinogenesis: from pathways to diagnosis and therapy studies. *J Carcinog* 2011;10:9.
36. Oancea I, Movva R, Das I, Aguirre de Carcer D, Schreiber V, Yang Y, Purdon A, Harrington B, Proctor M, Wang R, Sheng Y, Lobb M, Lourie R, P OC, Duley JA, Begun J, Florin TH. Colonic microbiota can promote rapid local improvement of murine colitis by thioguanine independently of T lymphocytes and host metabolism. *Gut* 2017;66:59–69.
37. Oancea I, Png CW, Das I, Lourie R, Winkler IG, Eri R, Subramaniam N, Jinnah HA, McWhinney BC, Levesque JP, McGuckin MA, Duley JA, Florin TH. A novel mouse model of veno-occlusive disease provides strategies to prevent thioguanine-induced hepatic toxicity. *Gut* 2013;62:594–605.
38. Florin THJ, Wright JD, Jambhrunkar SD, Henman MG, Popat A. A well-tolerated and rapidly acting thiopurine for IBD? *Drug Discov Today* 2019;24:37–41.
39. Witty JP, McDonnell S, Newell KJ, Cannon P, Navre M, Tressler RJ, Matrisian LM. Modulation of matrilysin levels in colon carcinoma cell lines affects tumorigenicity in vivo. *Cancer Res* 1994;54:4805–4812.
40. Cherciu I, Barbalan A, Pirici D, Margaritescu C, Saftoiu A. Stem cells, colorectal cancer and cancer stem cell markers correlations. *Curr Health Sci J* 2014; 40:153–161.
41. Sarela AI, Macadam RC, Farmery SM, Markham AF, Guillou PJ. Expression of the antiapoptosis gene, survivin, predicts death from recurrent colorectal carcinoma. *Gut* 2000;46:645–650.
42. Trieb K, Lehner R, Stulnig T, Sulzbacher I, Shroyer KR. Survivin expression in human osteosarcoma is a marker for survival. *Eur J Surg Oncol* 2003;29:379–382.
43. Petherick KJ, Williams AC, Lane JD, Ordonez-Moran P, Huelsken J, Collard TJ, Smartt HJ, Batson J, Malik K, Paraskeva C, Greenhough A. Autolysosomal beta-catenin degradation regulates Wnt-autophagy-p62 crosstalk. *EMBO J* 2013;32:1903–1916.
44. Chuang SJ, Cheng SC, Tang HC, Sun CY, Chou CY. 6-Thioguanine is a noncompetitive and slow binding inhibitor of human deubiquitinating protease USP2. *Sci Rep* 2018;8:3102.
45. Graham TA, Weaver C, Mao F, Kimelman D, Xu W. Crystal structure of a beta-catenin/Tcf complex. *Cell* 2000;103:885–896.
46. de Boer NKH, Thiopurine Working G. Thiopurine therapy in inflammatory bowel diseases: making new friends should not mean losing old ones. *Gastroenterology* 2019;156:11–14.
47. Massey DC, Parkes M. Genome-wide association scanning highlights two autophagy genes, ATG16L1 and IRGM, as being significantly associated with Crohn's disease. *Autophagy* 2007;3:649–651.
48. Baars JE, Looman CW, Steyerberg EW, Beukers R, Tan AC, Weusten BL, Kuipers EJ, van der Woude CJ. The risk of inflammatory bowel disease-related colorectal carcinoma is limited: results from a nationwide nested case-control study. *Am J Gastroenterol* 2011; 106:319–328.
49. Gordillo J, Cabre E, Garcia-Planella E, Ricart E, Bernieto Y, Marquez L, Rodriguez-Moranta F, Ponferrada A, Vera I, Gisbert JP, Barrio J, Esteve M, Merino O, Munoz F, Domenech E, Disease EPotSWGICs, Ulcerative C. Thiopurine therapy reduces the incidence of colorectal neoplasia in patients with ulcerative colitis: data from the ENEIDA Registry. *J Crohns Colitis* 2015; 9:1063–1070.
50. Axelrad JE, Roy A, Lawlor G, Korelitz B, Lichtiger S. Thiopurines and inflammatory bowel disease: current evidence and a historical perspective. *World J Gastroenterol* 2016;22:10103–10117.
51. van Staa TP, Card T, Logan RF, Leufkens HG. 5-Aminosalicylate use and colorectal cancer risk in inflammatory bowel disease: a large epidemiological study. *Gut* 2005;54:1573–1578.
52. Bernstein CN, Nugent Z, Blanchard JF. 5-aminosalicylate is not chemoprophylactic for colorectal cancer in IBD: a population based study. *Am J Gastroenterol* 2011;106:731–736.
53. Tenbaum SP, Ordonez-Moran P, Puig I, Chicote I, Arques O, Landolfi S, Fernandez Y, Herance JR, Gispert JD, Mendizabal L, Aguilar S, Ramon y, Cajal S, Schwartz S Jr, Vivancos A, Espin E, Rojas S, Baselga J, Tabernero J, Munoz A, Palmer HG. Beta-catenin confers resistance to PI3K and AKT inhibitors and subverts FOXO3a to promote metastasis in colon cancer. *Nat Med* 2012;18:892–901.
54. Gavert N, Ben-Ze'ev A. Beta-Catenin signaling in biological control and cancer. *J Cell Biochem* 2007; 102:820–828.
55. Dieter SM, Ball CR, Hoffmann CM, Nowrouzi A, Herbst F, Zavidij O, Abel U, Arens A, Weichert W, Brand K, Koch M, Weitz J, Schmidt M, von Kalle C, Glimm H. Distinct types of tumor-initiating cells form human colon cancer tumors and metastases. *Cell Stem Cell* 2011; 9:357–365.
56. Mizushima N, Levine B. Autophagy in mammalian development and differentiation. *Nat Cell Biol* 2010; 12:823–830.
57. Sheng YH, Lourie R, Linden SK, Jeffery PL, Roche D, Tran TV, Png CW, Waterhouse N, Sutton P, Florin TH, McGuckin MA. The MUC13 cell-surface mucin protects against intestinal inflammation by inhibiting epithelial cell apoptosis. *Gut* 2011;60:1661–1670.
58. Dervieux T, Boulieu R. Simultaneous determination of 6-thioguanine and methyl 6-mercaptopurine nucleotides of azathioprine in red blood cells by HPLC. *Clin Chem* 1998;44:551–555.

59. Friesner RA, Banks JL, Murphy RB, Halgren TA, Klicic JJ, Mainz DT, Repasky MP, Knoll EH, Shelley M, Perry JK, Shaw DE, Francis P, Shenkin PS. Glide: a new approach for rapid, accurate docking and scoring—1: method and assessment of docking accuracy. *J Med Chem* 2004; 47:1739–1749.
60. Yu B, Huang Z, Zhang M, Dillard DR, Ji H. Rational design of small-molecule inhibitors for beta-catenin/T-cell factor protein-protein interactions by bioisostere replacement. *ACS Chem Biol* 2013;8:524–529.
61. Li J, Abel R, Zhu K, Cao Y, Zhao S, Friesner RA. The VSGB 2.0 model: a next generation energy model for high resolution protein structure modeling. *Proteins* 2011;79:2794–2812.

Received March 25, 2020. Accepted May 27, 2020.

Correspondence

Address correspondence to: Timothy Florin, MSc, MD, Mater Research Institute - University of Queensland, Translational Research Institute, 37 Kent Street, Woolloongabba, Brisbane, QLD 4102, Australia. or e-mail: tflorin@uq.edu.au; or Jakob Begun, PhD, MD, Mater Research Institute - University of Queensland, Translational Research Institute, 37 Kent Street, Woolloongabba, Brisbane, QLD 4102, Australia. e-mail: jakob.begun@mater.uq.edu.au.

Acknowledgments

The authors thank Prof Andrew Clouston (Envoi Pathology & Berghofer Queensland Institute of Medical Research) for reporting on liver sections, Prof Allison Pettit for providing the IHC reagents, and Dr Kuan Yan Wong, Dr Ran Wang, and Ms Rhea Menon for help with experiments. The authors also recognize the technical assistance of the TRI core facilities for histology, flow cytometry, and microscopy.

CRedit Authorship Contributions

Yong Hua Sheng (Conceptualization: Supporting; Data curation: Lead; Formal analysis: Lead; Investigation: Lead; Methodology: Equal; Validation: Supporting; Writing – original draft: Equal; Writing – review & editing: Supporting)

Rabina Giri (Investigation: Equal; Methodology: Supporting; Visualization: Supporting)

Julie Davies (Data curation: Supporting; Formal analysis: Supporting; Investigation: Supporting; Methodology: Supporting; Validation: Supporting)

Veronika Schreiber (Data curation: Supporting; Methodology: Supporting; Resources: Supporting; Validation: Supporting)

Saleh Yahya M. Alabbas (Investigation: Equal)

Ramya Movva (Investigation: Equal)

Yaowu He (Investigation: Supporting; Methodology: Equal)

Andy Wu (Methodology: Supporting; Supervision: Equal)

John Hooper (Supervision: Lead)

Brett McWhinney (Investigation: Supporting; Methodology: Lead)

Iulia Oancea (Conceptualization: Supporting; Visualization: Equal)

Gregor Kijanka (Supervision: Equal)

Sumaira Hasnain (Investigation: Supporting; Supervision: Equal)

Andrew Lucke (Formal analysis: Supporting)

David Fairlie (Supervision: Supporting)

Michael McGuckin (Funding acquisition: Supporting; Supervision: Equal; Validation: Supporting)

Timothy H. J. Florin (Conceptualization: Equal; Project administration: Equal; Writing – original draft: Equal; Writing – review & editing: Lead)

Jakob Begun (Conceptualization: Lead; Funding acquisition: Lead; Project administration: Equal; Writing – original draft: Supporting; Writing – review & editing: Equal)

Conflicts of interest

The authors disclose no conflicts.

Funding

The Translational Research Institute (TRI) is supported by a grant from the Australian Government. Mater Research Institute is supported by Mater Foundation. JB has a UQ Reginald Ferguson Fellowship. AJL is supported by an ARC grant and DPF by the NHMRC.